Remote sensing of spatial variability in aeolian dune and interdune morphology in the Rub' Al-Khali, Saudi Arabia

Mohammed A. Al-Masrahy[1*] & Nigel P. Mountney[1]

1 – Fluvial & Eolian Research Group, School of Earth and Environment, University of Leeds, Leeds, LS2 9JT, UK * – corresponding author; email eemaa@leeds.ac.uk; Tel. +44 (0)7721073690

Abstract

The Rub' Al-Khali aeolian sand sea of south eastern Saudi Arabia – also known as the Empty Quarter – covers an area of 660,000 km² and is one of the largest sandy deserts in the world. The region is covered by the latest generation of public-release satellite imagery, which reveal spatially diverse dune patterns characterized by a varied range of dune types, the morphology, scale and orientation of which change systematically from central to marginal dune-field areas where non-aeolian sub-environments become dominant within the overall desert setting. Analysis of geomorphic relationships between dune and interdune sub-environments within 4 regions of the Rub' Al-Khali reveals predictable spatial changes in dune and interdune morphology, scale and orientation from the centre to the outer margins of dune fields. A quantitative approach is used to characterize the complexity present where large, morphologically complex and compound bedforms gradually give way to smaller and simpler bedform types at dune-field margins. Parameters describing bedform height, spacing, parent morphological type, bedform orientation, lee-slope expression, and wavelength and amplitude of along-crest sinuosity are recorded in a relational database, along with parameters describing interdune size (long- and short-axis dimensions), orientation, and style of connectivity. The spatial rate of change of morphology of aeolian sub-environments is described through a series of empirical relationships. Spatial changes in dune and interdune morphology have enabled the development of a model with which to propose an improved understanding of the sediment system state of the modern Rub' Al-Khali desert sedimentary system, whereby the generation of an aeolian sediment supply, its availability for aeolian transport and the sand transporting capacity of the wind are each reduced in dune-field margin areas.

Keywords: aeolian dune; interdune; desert; sand sea; dune field

Introduction

Significant advances in our understanding of the spatial arrangement of aeolian dune patterns have been made possible through the increasing availability of high-resolution satellite imagery in recent years (e.g. Blumberg, 2006; Hugenholtz and Barchyn, 2010). Aeolian dune-field patterns are a product of self-organizing systems (Kocurek and Ewing, 2005; Wilkins and Ford, 2007; Ewing and Kocurek, 2010a) in which the development of simple or complex distributions of genetically related groups of aeolian bedforms and their adjoining interdunes is characterized by systematic and predictable changes in dune type, size, morphology, orientation and spacing from dune-field centre to dune-field margin settings (Werner and Kocurek, 1997, Kocurek and Ewing, 2005; Ewing et al. 2006; Bullard et al. 2011).

Several previous studies have documented spatial variation in bedform type and associated spatial changes in aeolian lithofacies distributions in desert dune fields (e.g. Breed & Grow, 1979; Sweet et al., 1988; Kocurek and Lancaster, 1999; Atallah and Saqqa, 2004; Baas, 2007; Bullard et al. 2011). However, relatively few studies have attempted to quantitatively document the form of spatial variability of dune and interdune morphology from the centres of aeolian dune-field systems to their margins (Kocurek and Ewing, 2005; Wilkins and Ford, 2007; Ewing and Kocurek, 2010a, b; Kocurek et al. 2010; Hugenholtz and Barchyn, 2010).

This study utilizes the latest generation of public-release satellite imagery to quantify the form of geomorphic relationships between dune and interdune sub-environments in both the central and marginal parts of four modern dunes fields of the Rub' Al-Khali (Empty Quarter) of Saudi Arabia. The overall aim of this work is to document how and explain why dune- and draa-scale aeolian bedforms and their adjoining interdunes systematically change form from central to marginal dune-field areas in terms of their morphology, geometry (scale), orientation and style of bedform linkage (i.e. the extent to which interconnected and amalgamated aeolian bedform complexes are developed). Specific objectives of this research are as follows: (i) to assess the geomorphic complexity and variety of dune types present in the Rub' Al-Khali desert; (ii) to demonstrate and quantify styles of spatial variation in dune and interdune type and geometry for a series of major dune fields; (iii) to consider how a series of external factors that collectively define the sediment state of the system act to dictate spatial changes in dune and interdune morphology and geometry.

This research is important because understanding the morphology and architectural distribution of the deposits of aeolian dune and interdune sub-environments serves to constrain the development of models with which to explain the principal controls on desert dune distributions. Further, the establishment of spatial trends in dune morphology and geometry aids the reconstruction of ancient aeolian palaeoenvironments and guides the prediction of sedimentary architecture in subsurface stratal successions. Understanding the morphological complexity present in a range of modern aeolian desert systems is a primary control on preserved stratigraphic complexity and is the first step in developing a series of generic models with which improve our understanding of the mechanisms by which complex sedimentary architectures arise in ancient preserved aeolian successions. Thus, there exists a need to document the morphology of modern desert systems to understand how spatial morphological changes in dune type and size might impact preserved stratigraphic architecture (Mountney, 2012).

Background

Modern aeolian dune-field systems are composed of complex arrangements of geomorphic elements, including dunes, draa and interdunes, which occur on a range of scales and are characterized by a variety of morphologies and geometries (Warren and Knott, 1983; Kocurek and Havholm, 1993; Lancaster, 1994; Rubin and Carter 2006; Ewing and Kocurek, 2010a). In many dune-field systems, the form of geomorphic elements and their relationship with adjacent elements varies systematically and predictably as a function of position within the overall aeolian system, especially in downwind directions and from the centre to outer margins of dune fields (Breed et al. 1979; Lancaster, 1983, 1994). Indeed, groups of genetically related aeolian dunes and intervening interdunes represent some best examples of patterned landscapes in nature (Kocurek and Ewing, 2005).

Few aeolian desert sand dunes exist in isolation. Most cluster, with many examples forming large dune fields in which systematic patterns of groups of genetically related dunes can be recognized, in some cases repeating with spatial regularity or with one or more defining attribute of the dune-form changing progressively in a given direction from, say, the centre of a dune field to its margin. Groups of dunes collectively form larger geomorphic elements typically referred to as sand seas, dune fields (Livingstone and Warren, 1996) or ergs (Wilson, 1973). Although Cooke et al. (1993) define the lower size limit for a sand sea at 30 000 km^2, this being an inflexion point on the distribution curve of sand-sea size given by Wilson (1973), in modern usage (post-1995), no lower size limit is formally applied by way of definition.

Dune fields are not necessarily continuously covered with active aeolian sand dunes and most additionally include other morphological bodies of aeolian-derived or aeolian-related sediment deposits, including interdunes, sand sheets (which lack distinctly recognizable larger bedforms), areas of soil cover, lacustrine systems (e.g. playa lakes), and fluvial systems (typically ephemeral), some developed between active aeolian dunes (Lancaster, 1989). Thus, dunes in sand seas, including those in the Rub’ Al-Khali, are commonly separated from each other by geomorphic elements whose well-defined shapes are, in part, dictated by the shapes of adjoining dune bedforms of different types (e.g. McKee and Bigarella, 1979).

The construction of aeolian dune-field systems and the spatial variation in the form of their internal components (e.g. dunes and interdunes) from central to marginal areas is governed by numerous controlling parameters that dictate sediment state (Berg, 1986; Kocurek, 1998, 1999; Kocurek and Lancaster, 1999). At a regional scale, the sediment state of aeolian dune fields is defined by separate components of sediment supply, sediment availability and transport capacity of the wind (Kocurek and Lancaster, 1999), and together these factors govern where and when aeolian system construction via the growth of dunes occurs.

Study area

The Rub’ Al-Khali of south-eastern Saudi Arabia – also known as the Empty Quarter – is one of the largest continuous sand deserts in the world and comprises a series of dune fields, some spatially discrete and some merging into neighbouring fields, within which self-organised patterns of aeolian bedforms and adjoining interdunes are developed (Bishop, 2010). The name for the Arabian desert – Rub’ Al- Khali or the Empty Quarter – was introduced by the Swiss geographer Burckhardt (1829) in his book "Travels in Arabia" and used later by Doughty (1888). Early research by Thesiger (1949), Beydoun (1966), Holm (1960, 1968), Glennie (1970) and Breed et al. (1979) each documented the presence of different bedform types and noted general spatial variations in dune types between different parts of the overall desert system.

In total, the Rub' Al-Khali covers approximately 660,000 km^2, rising to 776,000 km^2 of continuous active sand cover if adjoining sand seas (e.g. Jafura, Dahna and Nefud in Saudi Arabia) are additionally included (Breed et al. 1979, Edgell, 1989, 2006). Indeed, the wider desert region, which additionally incorporates the Wahiba Sand Sea of the Sultanate of Oman (Laity, 2009), covers an area of 795,000 km^2. Within the main the Rub' Al-Khali, active aeolian dunes and interdunes cover an area of 522,340 km^2 (Edgell, 2006), extending from United Arab Emirates and Oman in the east, to south-western Saudi Arabia and northern Yemen (Figure 1; Wilson, 1973, Glennie, 2005, Edgell, 2006). The largely unconsolidated sand dune deposits of the Rub' Al-Khali are characterized by large bedforms (dunes and draa), individual examples of which range from 50 to 300 m in height (Brown et al. 1963; Abd El Rahman, 1986; Edgell, 2006), and the majority of which are each separated by broad interdune flats, some up to 5 km in width in dune-field margin settings (Figure 2). The majority of the Quaternary sediments of the Rub' Al- Khali are composed chiefly of aeolian-reworked Pliocene alluvial sediments (McClure, 1978), though a secondary sand component is likely to have been additionally sourced from local modern alluvial (wadi) sediments (Holm, 1960; Brown, 1960).

The Rub' Al-Khali basin is a combined physiographical and tectonic feature (Bagnold, 1951; Powers et al., 1966; McClure, 1976, 1978; Edgell, 1989, and Clark, 1989) that forms a structural depression characterized as an embayment with a structural axis trending from northeast-to-southwest, bordered to the northwest and west by the Arabian Shield, and to the south and southeast by the Hadramawt-Dhofar Arch or Plateau (Figure 1b). The northern end of Rub' Al-Khali basin opens into the Arabian Gulf through the United Arab Emirates (Edgell, 2006). The desert is additionally constrained by the arc of the Oman Mountains to the northeast and by the Qatar Arch to the northwest (Figure 1b). The area occupied by active sand seas extends from the United Arab Emirates and Oman in the east, to south-western Saudi Arabia and the area directly north of Yemen.

Quaternary evolution of the Rub' Al-Khali

The Rub' Al-Khali formed in response to cyclic episodes of aridity driven by climatic fluctuations throughout much of the Quaternary period (Edgell, 1989, 2006; Glennie, 1998; Goudie, et al. 2000). The application of optical dating methods to sand samples from both linear and crescentic dunes has demonstrated that the majority of the dunes of the Rub' Al-Khali formed during cold, arid intervals associated with high latitude Quaternary glacial cycles and concurrent sea-level lowering (Glennie, 1998; Glennie and Singhvi, 2002; Preusser et al., 2002; Lancaster and Tchakerian, 2003; Edgell, 2006; Bishop, 2010). Most dune fields of the Rub' Al-Khali were more extensive than their present-day distribution during earlier parts of the Quaternary (Pye and Tsoar, 2009), though were less extensive than at present during the middle Holocene (Sarnthein, 1978). Indeed, the evolution of the Rub' Al-Khali is known to have been influenced by climatic changes from arid, to semi-arid, to sub-humid throughout much of the Quaternary, with changes in mean annual precipitation and wind direction (Anton, 1984), and changes in sea level (Lancaster, 1998;) each exerting a control on landscape evolution.

Dunes of the Rub' Al-Khali (and indeed other deserts of the Arabian Peninsula) underwent several phases of spatial and temporal evolution in response to Quaternary climate and environmental change (Alsharhan et al., 1998, 2003; Anton, 1984, 1985; Hotzl et al., 1978). Firstly, an increase in aridity, especially during the late Pleistocene, encouraged the construction of dune fields whereby the availability of sediment for aeolian transport and regional variation in wind directions governed dune morphology such that complex dunes and draa developed. Secondly, increased climatic humidity during the early Holocene enabled lakes to develop and vegetation cover to partly stabilize the substrate, thereby restricting the availability of sediment for aeolian transport, limiting further dune construction, encouraging partial deflation in areas where the sand carrying capacity of the wind was undersaturated with respect to its potential, and encouraging the growth of non-aeolian regions. Some of the larger compound bedforms present in the Rub' Al- Khali (e.g. those in the Liwa area of the United Arab Emirates) are known to have been constructed in response to the effects of repeated Quaternary climatic changes whereby multiple generations of superimposed dunes are delineated by calcrete horizons that record repeated episodes of bedform construction, partial deflation and stabilization indicative of alternations between relatively arid and relatively more humid climatic conditions (El-Sayed, 1999, 2000).

Throughout much of the Quaternary, spatial and temporal changes in dune morphology and geometry, and their spatial relationships are known to have been controlled significantly by changes in position, direction and intensity of Shamal and Indian Ocean Monsoon wind regimes (Preusser, 2009). The Shamal wind is a hot and dry wind with substantial sand-transporting capacity (Barth, 2001; Edgell, 2006) that forms as part of a large-scale flow of air toward a low-pressure centre that develops over Pakistan each year (Edgell, 2006). Although active in both summer and winter, it is most intense in June and July when it blows almost continuously at velocities that commonly reach and exceed 50 km h^{-1}. These winds are the principal agent for aeolian transport of sand and dune formation in much of the Arabian Peninsula (Membery, 1983).

Data and Methods

This study has entailed work in four distinct geographic areas of the Al Rub' Al-Khali, herein called Areas 1, 2, 3 and 4 (Figure 2a), which collectively cover an area of 73,200 km^2. These areas were selected for study according to the following specific criteria: (i) chosen locations document spatial changes in the morphology of dunes and interdunes from the central part of a dune field to its outer margin; (ii) public-release satellite imagery used for examination of the dune forms is available for these areas at a resolution that is sufficiently high to enable detailed quantitative measurements to be made regarding various morphological attributes of dunes and interdunes.

Morphological and geometrical attributes relating to 555 dunes and 1415 interdunes from the 4 selected study areas were collected through examination of satellite imagery provided by Google Earth Pro software and datasets, a business- and scientific-oriented mapping service (Figure 3). Satellite imagery from the studied areas has a spatial resolution of resolution 15 m per pixel, derived from 15 to 30 m-resolution multispectral Landsat data that have been pan-sharpened with panchromatic Landsat image processing software. Individual high-resolution images are each 4800 x 2442 pixels and images recording adjacent areas have been seamlessly tiled to render larger visualizations of each study area. Elevation data are derived from Shuttle Radar Topography Mission (SRTM) data, which has an absolute vertical accuracy of 16 m and a relative vertical accuracy of 10 m (Falorni et al., 2005).

Collected dune and interdune data have been recorded in a relational database and this has been used to discern trends between measured parameters. Spatial variation in both dune and interdune size and shape in directions both close to parallel and close to perpendicular to the overall direction of net sand transport has been recorded, with the resultant net direction of sediment transport having been identified from the analysis of dune bedform type and slipface orientation and through reference to Resultant Drift Direction calculations made by Fryberger & Dean (1979).

Attributes recorded for dunes are as follows and as depicted in Figure 4: bedform height is based on relief change from the regional level of the desert surface indicated by the elevation of interdune flats in the outer dune-field margin area to the crests of the bedforms; the along-crest length of a dune segment is a measure of bedform continuity whereby dune segments are terminated by major re-entrants or scours; bedform spacing is the crest-to-crest (or toe-to-toe) distance between adjacent bedforms in an orientation perpendicular to the trend of elongate bedform crestlines; dune wavelength records the extent of a bedform in an orientation perpendicular to the trend of the bedform crestline and this may vary from a maximum dune wavelength to a minimum dune wavelength within one dune segment as a function of bedform sinuosity; the wavelength and the amplitude of along-crest sinuosity observed in plan form together define crestline sinuosity (Rubin, 1987); bedform long-axis orientation describes the trend of dune crestlines; the distance from the dune-field centre is a relative measure of distance from the centre of the studied dune fields to their outer margins. Attributes recorded for interdunes are as follows and as depicted in Figure 4: interdune length is a measure of the distance that a single interdune corridor extends in an orientation parallel to the trend of the crestlines of the dunes that bound the interdune; interdune width is a measure of the width of an interdune flat developed between two dunes in an orientation perpendicular to interdune length; interdune long-axis orientation describes the trend of an interdune; the distance from the dune-field centre is a relative measure of distance from the centre of the studied dune fields to their outer margins.

The terminology applied in this study is derived from that introduced by Rubin (1987) and that used in a slightly modified form more latterly by a variety of authors including Mountney and Thompson (2002), Rubin and Carter (2006) and Mountney (2006, 2012). It is important to note that some authors view the term "bedform wavelength" to be synonymous with "bedform spacing" (cf. Breed and Grow, 1979) but for the purposes of this study, and also as used by the aforementioned authors, the two terms differ in that bedform wavelength defines the distance from the leeward toe to the rearward (stoss) toe of the bedform in an orientation parallel to the direction of downwind migration. By contrast, bedform spacing defines the crest-to-crest (or toe-to-toe) distance from one bedform to an adjacent bedform, again in an orientation parallel to the direction of downwind migration. Thus, bedform spacing additionally incorporates the size of any adjoining interdune flat present between two bedforms (Figure 4).

Further to the wind directional data documented by Fryberger & Dean (1979), additional data relating to wind direction were obtained for the period 1982 to 2013 from 5 stations located in the central and eastern parts of the Rub' Al-Khali and these indicate a prevailing Resultant Drift Direction to the southwest (Figure 5).

Dune morphology in the Rub' Al-Khali

Satellite imagery for the Rub' Al-Khali reveals a varied range of dune types, the morphology of which changes systematically from central dune-field areas to marginal areas where ephemeral fluvial systems become dominant (Figure 2b). The spatial variability of the dunes and interdunes present in this desert region is significant and was the principal reason for the choice of this region for this study. Key attributes describing the nature of the dunes and interdunes present in the studied areas are are summarised in Tables 1 and 2.

Although aeolian dune forms in the Rub' Al-Khali are many and varied, three principal forms are defined at a fundamental level: transverse, linear and star forms, depending on whether the orientation of dune crest-lines is close to perpendicular or close to parallel to the dominant wind direction, or whether the forms exhibit a multi-facetted, pyramid-like morphology, respectively (Figure 6; Hunter et al., 1983; Kumar and Mahmoud, 2011). These fundamental bedform types are broadly distributed into three regions, as identified by Breed et al*.* (1979) through their analysis of Landsat imagery and Skylab photographs, and as summarized by Glennie (2005): crescentic transverse dunes dominate in the northeast part of the study region, linear dunes dominate throughout the western half, and star dunes dominate along the eastern and southern margins (Figure 2b; cf. Glennie, 1970). Additionally, zones occupied by non-classified complex dune forms and sand sheets and streaks are also recognized (Breed et al*.*, 1979). Edgell (1989) used Landsat 7 near-infrared imagery, large-format camera images and field observations to divide the three primary bedform classes into 17 specific bedform types, though for this study the basic three-fold classification is used for the sake of simplicity.

Compound crescentic transverse dunes – some termed 'giant crescentic massifs' and 'compound crescentic dunes' (Breed and Grow, 1979; Breed et al*.*, 1979) – in the northern and eastern Rub' Al-Khali, including in the Uruq al Mutaridah sub-basin (Figure 2b, c; Glennie, 2005), have a mean horn-to-horn width of 2.8 km, a mean length of 2.1 km (cf. Breed et al*.*, 1979) and exhibit a vertical relief of up to 160 m above the surrounding desert floor that is characterised by interdune flats and up to 230 m above sea-level datum (Figure 7). A 'hooked' variety of compound crescentic dune is described from the north-central and northeastern Rub' Al-Khali (Breed and Grow, 1979; Holm, 1960). Compound linear dunes in the western and south-western Rub' Al-Khali are aligned from northwest to southeast, parallel to Shamal winds (Glennie, 2005), and have different types of smaller dunes including star and barchan forms superimposed on them (Breed and Grow, 1979). These linear forms have a mean dune spacing of 3.9 km, are in places in excess of 130 m high above the surrounding desert floor that is characterised by interdune flats and up to 200 m above sea-level datum; they form linked chains of bedforms, some of which extend uninterrupted for distances up to 50 km (Figures 6c and 8, transect I-I'; Bunker,1953; Holm, 1960; Breed et al*.*, 1979). Neighbouring linear bedforms are separated by interdune flats (see below) that themselves each have a mean width of up to 1.4 km. Bedforms at the eastern and south-eastern margin of Rub' Al-Khali are mainly star dunes with mean widths of 2.1 km and heights up to 120 m above the surrounding desert floor that is characterised by interdune flats (Figures 6d and 8, transect J-J'); these types merge with barachanoid dunes forming complex bedforms with slipfaces generally oriented toward the southeast (McKee and Breed, 1976).

The majority of dunes in the studied sand seas are separated from each other by extensive interdune-flat areas whose shapes are at least partly dictated by the morphology of adjoining dunes of different types (cf. McKee, 1979). Interdunes in the Rub' Al-Khali vary in shape and in size (Figure 6), with the size and continuity typically increasing toward the margins of the dune fields (Figure 7), where the supply of sand and its availability for aeolian bedform construction is less, especially in areas where the water table lies close to the accumulation surface, such that the draw-up of moisture form the shallow subsurface via capillary action leaves the surface damp, thereby encouraging adhesion of sand (cf. Kocurek and Fielder, 1982; Olsen, et al. 1989). Open interdune corridors vary in length from 0.5 km in the central parts of dune fields to in excess of 50 km at dune-field margins; widths vary from 0.2 to 6 km.

Morphological and geometrical relationships between dunes

Dune bedform wavelength is a simple measure of bedform size herein defined as the extent of a dune bedform in an orientation perpendicular to its crestline. In this study both maximum and minimum dune wavelength are recorded for individual dune segments (Figure 4) as a measure of size. The difference between maximum and minimum wavelength for a single dune segment is also a measure of along-crest crest variability, with similar values representing relatively straight-crested bedforms and values with greater differences reflecting increasing bedform crestline sinuosity (cf. Rubin, 1987; Rubin and Carter, 2006). A strong positive correlation exists between maximum and minimum dune wavelength (Figure 9a). Dunes from all areas exhibit a decrease in mean dune wavelength with increasing distance away from the dune-field centre and towards the outer margin (Figure 9b). Combined results from all 4 study areas demonstrate that over a distance of 300 km average dune wavelength decreases from 1.5 km at the dune-field centre to ~0.1 km at the dune-field margin.

Dune spacing is the distance between successive dunes in a train (measured, for example, between successive bedform crests), and includes both the wavelength of a dune bedform plus the width of the adjoining interdune (Figure 4). In contrast to dune wavelength, dune spacing exhibits little or no change with increasing distance from a dune-field centre toward its margin (Figures 7 and 9c), though recorded values of dune spacing demonstrate considerable spread and vary mainly between 2 and 4 km. Given the lack of discernible change in mean dune spacing from the central parts of the dune fields to their margins, yet the systematic decrease in mean dune wavelength (i.e. bedform size), progressively smaller bedforms in dune-field margin settings are compensated for by progressively wider interdunes.

Wavelength and amplitude of along-crest plan-form sinuosities are together a simple measure of bedform crestline sinuosity (Rubin, 1987). For each of the 4 study areas, over a distance of 300 km, mean amplitude of along-crest sinuosity decreases from 2.5 km at the centre of dune field to less than 0.5 km at the outer margin where the dunes become smaller (Figure 9d). Mean wavelength of along-crest sinuosity decreases from 5 km at the dune-field centre to ~0.2 km at the dune-field margin (Figure 9e). A positive relationship between dune along-crest amplitude and wavelength demonstrates little change of the form of along-crest sinuosity across the dune field (Figure 9f).

Bedform height (defined as the difference in relief between the crest of a bedform and the general level of the desert surface where interdune flats are present) varies as a function of both bedform type and location within the dune field in terms of proximity to the outer dune-field margin (cf. Lancaster, 1988). Data collected from this study reveal bedforms with heights that range from <5 m at the dune-field outer margin to >155 m in the dune-field centre. The relationship between bedform height and spacing is complex (Figure 10a) and reveals no predictable trend because dune spacing is largely independent of bedform size. By contrast, a positive correlation exists between bedform height and wavelength (Figure 10b), though the spread in these data likely reflect contrasts between dunes of fundamentally different morphological types. Although bedform height generally decreases from the dune-field centre to its outer margin (Figure 10c), the trend is not straight-forward because bedforms tend to undergo changes in morphology along such transects.

Morphological and geometrical relationships between interdunes

The relationship between interdune long-axis length and width exhibits a positive correlation (Figure 11a), with the rate of increase of length relative to that of width being largely independent of the study area. Interdunes have a tendency to become longer and wider with increasing distance from a fixed point in the dune-field centre towards the eastern dune-field margin (Figure 11b, c), though considerable variability exists. For the data from Area 3, as interdune lengths become very large (> 40 km) their widths stabilize at 1.5 to 3.5 km in the dune-field margin areas (Figure 7, Section C-C'; Figure 11c). In these marginal areas, interdunes become the dominant landform type and they effectively partition the dune field with the dune bedforms being subordinate and in some cases spatially isolated landforms. Considering the entire dataset, interdune long-axis orientation systematically varies (mimicking the trend of bedform crestlines); interdune long-axes rotate systematically counter-clockwise from ~130-310 degrees in the central dune-field areas to 070-250 degrees at the dune-field margin, 300 km away (Figure 11d). Two dominant orientation trends are evident: interdunes in Areas 1, 2 and 3 are mostly oriented between 0 and 200 degrees, with a cluster of interdunes trending between 050 and 130 degrees; in Area 4 interdunes have long-axis orientations preferentially trending between 200 and 300 degrees (Figure 11d). The spatially isolated interdune depressions present between bedforms in the central dune-field region are elevated up to 25 m above the regional level (Figures 7 and 10d) and this demonstrates that bedforms in these central regions are climbing over one another to generate an accumulation. The elevation of interdunes in Area 4 is ~20 m higher than that in Areas 1-3 (Figures 7 and 10d) because bedforms and interdunes in this most southerly study area are constructed on a topographically elevated basement.

Discussion

Use of satellite imagery for the analysis of changes in morphology, geometry, orientation and related attributes of dunes and interdunes present along a series of transects from central to marginal positions within 4 areas of the Rub' Al-Khali represents a quantitative approach to the characterization of the changing spatial distribution of aeolian geomorphic elements and sub-environments in desert settings. The observed spatial variation in patterns of dune bedform and interdune arrangement arise as a consequence of several controls that operate to determine aeolian sediment system state in the studied dune fields. Although results from the analysis of this dataset do not necessarily enable quantitative determination of the nature of these controls, they do allow for the statement of a series of generalised discussion points.

Relationships between dune wavelength, interdune length and width, and position in the dune field highlight how interdune morphology interacts with the spatial distribution of dunes. The increase in interdune size and connectivity in dune-field margin areas and the corresponding decrease in dune size results from an overall reduction in either (i) the rate of generation of a sand supply for aeolian bedform construction in dune-field margin settings, (ii) the availability of that supply for aeolian bedform construction, or (iii) a downwind reduction in the sediment transport capacity of the wind (Kocurek and Lancaster, 1999). In dune-field margin settings, where areas of interdune flats are dominant, supply-limited and availability-limited aeolian systems are common and are controlled by factors such as the presence of a damp substrate due to an elevated, near-surface water table (e.g. Hotta et al., 1984) and/or the action of surface-stabilizing agents such as vegetation and precipitated crusts (e.g. Glennie, 2005; Edgell, 2006; Kumar and Mahmoud, 2011). Downstream reduction in the transport capacity of the wind at dune-field margin may also limit potential for dune construction (e.g. Ash and Wasson, 1983; Anderson and Haff, 1991). The presence of a near-surface water table in the outer margins of the studied dune fields such that its capillary fringe acts as a wicking effect to maintain a damp surface effectively renders these parts of the study area wet aeolian systems (*sensu* Kocurek and Havholm, 1993) such that, although a source of sand-grade sediment that is potentially suitable for aeolian transport and dune construction may be present within interdune flats, this supply is not available for transport. Thus, water-table level plays a fundamental role in limiting dune construction and protecting interdune flats from deflation. Indeed, a progressive rise in the relative level of the water table in the outer dunefield margin areas may potentially enable accumulation of packages of interdune strata between the accumulations of migrating dunes (cf. Mountney and Russell, 2006, 2009).

The positive correlation between interdune length and width, and distance from a fixed point in the dune-field centre, which summarizes the form of generalised changes in dune and interdune morphology across the dune field, arises as a result of a change in the sediment state components. The relations reveal significant geomorphological changes in the interdune areas and adjoining dunes across the dune field, and these represent a systematic spatial reduction in sediment supply and availability for aeolian transport, most likely because sediment is stored in upwind, central parts of the dune field rendering the wind undersaturated with respect to its potential sand transporting capacity in downwind dune-field margin areas, and therefore potentially capable of sediment deflation.

Dunes in the Rub' Al-Khali desert exist in great variety of morphologic types that change systematically across the dune field. Variation in dune form is the primary control on the morphology of adjacent interdunes, especially in dune-field centre regions where the shape and extent of each interdune form is governed and defined by the geometry and spacing of surrounding dune forms.

Spatial variation in the arrangement of dune patterns in the Rub' Al-Khali takes the form of gradational transitions from complex to simple bedform types, and a decrease in dune size and an associated increase in interdune size from the centre to the outer-margin areas of dune fields. Such changes reflect the interaction between sediment supply and transport capacity. The availability of sand for dune construction has long been recognised as a primary control on dune morphology (e.g. Wilson, 1972), whereby simple barchan dunes tend to evolve in systems where sand supply is limited and therefore are the main bedform type in marginal areas of many dune fields including the eastern part of the Rub' Al-Khali studied here. By contrast, the central and northern part of the studied dune field is dominated by interlinked barchanoid dune types, whose presence records a greater sand supply.

Interdune orientation varies systematically as a function of geographic location, which in turn reflects the distribution and form of surrounding dunes, development of which is governed by prevailing wind type, directionality and intensity (Resultant Drift

Potential and Resultant Drift Direction) and seasonality (Fryberger and Dean, 1979). Study Area 1, which is located in the northeast of the Rub' Al-Khali, is dominated by large linked barchanoid dune ridges; Study Area 4, which is located in the southeast of the Rub' Al-Khali, is characterized by a systematic change from connected to isolated star dunes and associated changes in interdune morphology whereby the observed dune-form variability arises partly because of low length-to-width ratios of the dune wavelength. The direction and the rate of aeolian sand transport are strongly governed by the wind regime, velocity and direction (cf. Pye and Tsoar, 2009). Data depicting dune cross-sectional morphology (Figure 7) demonstrate increasing variability in the range of bedform height and spacing in several marginal dune-field areas (e.g. transects C-C' and D-D'), which likely results from a sediment state that is not in equilibrium for these parts of the studied system.

The Rub' Al-Khali region is influenced by winds with a high drift potential (the energy of surface winds in term of their capability to induce sand transport), chiefly because of the action of trade winds in mid-latitude depressions (Fryberger and Ahlbrandt, 1979). Directional variability of effective winds – south-southwest in winter and northwest in spring and summer (the so-called Shamal wind) – influences both the sand transporting potential of the wind (and therefore the bedform migration rate) and the Resultant Drift Direction (itself a control on dune migration direction) in the Rub' Al-Khali. This explains the high system activity and the pronounced variety of bedform patterns, sizes and orientations. Unidirectional winds are responsible for the construction of large crescentic (barchan) dunes, which attain heights in excess 130 m in some areas in northern part of the dune field. Seasonally varying Shamal winds form linear dune ridges; more complex multi-directional winds form the star dune complexes that dominate in the southern part of the dune field.

The extracted elevation data describing surface topography, which were acquired as a series of transects recording changes in dune spacing, height and morphology from different locations and in different orientations across the study areas (Figures 7 and 8), show clear examples of dune and interdune variability in the Rub' Al-Khali sand sea. The central part of the dune field contains the largest and most connected dune forms, many of which exceed 130 m in height (up to 160 m high), and this reflects bedform construction enabled by a large sand supply. Transects in Figure 7 each show spatially isolated interdune depressions within the central dune-field regions that are elevated up to 25 m above the regional level and this demonstrates that bedforms in these central regions are climbing over one another to generate an accumulation whereby the general interdune level is elevated above the regional level of the desert floor observed in more marginal dune-field areas (Figure 10d; *sensu* Kocurek, 1999).

In transects oriented in an upwind-to-downwind direction located in more central parts of the dune field (e.g. transects E-E' and F-F', Figures 2a and 8) no discernible downwind change in mean bedform height, wavelength or spacing is evident. By contrast, in transects oriented in an upwind-to-downwind direction but located in the zone of transition between the central and marginal parts of the dune field (e.g. transects G-G' and H-H', Figures 2a and 8), a general reduction in dune height and wavelength (Figures 9b and 10c), and an associated increase in interdune width (Figure 11c) in a downwind direction are evident and such changes are indicative of a spatial reduction in the availability of sand for bedform construction in downwind dune-field margin regions.

Conclusions

The latest generation of high-resolution, public-release satellite imagery and SRTM digital elevation data has provided the basis for a quantitative analysis of patterns of arrangement of large-scale aeolian bedforms and adjoining interdunes in a series of large sand seas present as desert dune fields in the Rub' Al-Khali of south-eastern Saudi Arabia. Image analysis documents a varied range of dune types, the morphology of which changes systematically from central dune-field areas to marginal areas where aeolian interdunes, sand sheets, and ephemeral fluvial systems dominate. Analysis of geomorphic relationships between dune and interdune sub-environments within 4 modern dune fields documents how dune and interdune morphology, geometry and orientation varies over space from dune-field-centre to dune-field-margin settings. Results demonstrate a characteristic reduction in aeolian dune size and degree of connectivity and a corresponding increase in interdune size and degree of connectivity towards outer dune-field margins. The collection of data relating to primary landform morphology has enabled an improved understanding of the sediment system state of the modern Rub' Al-Khali desert sedimentary system. Observed trends arise as a function of spatial changes in the sediment state of the system whereby sediment supply, the availability of that supply for transport and the sediment transporting capacity of the wind each combine to dictate the geomorphology of dune and interdune forms, which vary from thick accumulations of sands in the form of coalesced compound and complex barchanoid bedforms in dune-field centre settings, to spatially discrete star dunes and small, spatially isolated barchan dunes separated by extensive water-table-controlled interdune flats in dune-field margin settings. Observations from this modern dune-field system have enabled the spatial rate of change of morphology of aeolian sub-environments to be characterized and described through a series of empirical relationships.

Results of this study have implications for developing an improved understanding of the likely controls on the detailed sedimentary architecture of preserved aeolian successions by enabling the proposition and development of a range of dynamic facies models for aeolian systems. This has wider applied implications and significance: for example, the morphological changes in the distribution of aeolian bedforms and interdunes across dune-field systems provides important information with which to improve our understanding of the likely arrangement of architectural elements in ancient aeolian preserved successions, several of which form important reservoirs for hydrocarbons. This work is therefore an important step in the development of improved models for the characterisation of stratigraphic complexity and heterogeneity in aeolian reservoirs.

Acknowledgements

We are grateful to Editor Juan Pedro Rodríguez-López and to two anonymous reviewers for their constructive recommendations on how to improve this manuscript. MAM is grateful to Saudi Aramco for their sponsorship of this research programme. Areva, BHPBilliton, ConocoPhillips, Nexen, Saudi Aramco, Shell, Tullow Oil and Woodside are thanked for their sponsorship of the wider FRG-ERG research programme at the University of Leeds, of which this study forms a part.

References

Abd El Rahman, A. A., 1986. The deserts of the Arabian Peninsula, in: M. Evenari, I. Noy-Meir, Goodall, D.W (Eds.), Ecosystems of the World 12B-Hot Deserts and Arid Shrublands. Elsevier, Amsterdam, pp. 29-54.

Alsharhan, A.S., Glennie, K.W., Whittle, G.L., Kendall, C.G., 1998. Quaternary deserts and climate change. Proceedings of the International Conference on Quaternary deserts and climate change, Al Ain, UAE, December 9-11, 1995. A.A. Balkema. 621 p.

Alsharhan, A.S., Wood, W. W., Goudie, A.S., Fowler, A., Abdellatif, E.M., 2003. Desertification in the third millennium. Proceedings of an international conference, Dubai, February 12-15, 2000. A. A. Balkema.490 p.

Anderson R.S., Haff, P.K., 1991. Wind modification and bed response during saltation of sand in air. Acta Mechanica 1, 21-52.

Anton, D., 1984. Aspects of geomorphological evolution: paleosols and dunes in Saudi Arabia, in: R.A.Jado and Jotl, J. (Eds.), Quaternary Period in Saudi Arabia, Springer-Verlag, Wien, pp. 275-297.

Anton, D., 1985. Environmental changes and aeolian dynamics during the Quaternary in the Arabian Peninsula, in: El-Baz, F., El-Tayeb, I.A., Hassan, M.H. (Eds.), Proceedings of the International Workshop on "Sand Transport and desertification in Arid Lands", Khartoum, Sudan, World Scientific, Singapore, pp. 209- 234.

Ash, J.E., Wasson, R. J., 1983. Vegetation and sand mobility in the Australian desert dunefield. Z. Geomorphology 45, 7-25.

Atallah, M., Saqqa, W., 2004. Characterization of aeolian terrain facies in Wadi Araba desert, southwestern Jordan, Geomorphology 62, 63-87.

Baas, Andreas C., 2007. Complex systems in aeolian geomorphology, Geomorphology 91, 311-331.

Bagnold, R.A., 1951. Sand formations in southern Arabia. Geological Journal 117, 78-86.

Barth, H.J., 2001. Characteristics of the wind regime north of Jubail, Saudi Arabia, based on high resolution wind data, Journal of Arid Environments 47, 387-402.

Berg, R.R., 1986. Reservoir Sandstone, Prentice-Hall, Inc. Englewood Cliff, New Jercy 07632. 481p.

Beydoun, Z.R., 1966. Geology of the Arabian Peninsula – Eastern Aden Protectorate and part of Dhufar, U. S. Geological Survey Professional Paper, 560. Geological Society, London, Special Publication 49, 697–714.

Bishop, M.A., 2010. Nearest neighbor analysis of mega-barchanoid dunes, Ar Rub' Al- Khali, sand sea: The application of geographical indices to the understanding of dune field self-organization, maturity and environmental change. Geomorphology 120, 186-194.

Blumberg D.G., 2006. Analysis of large aeolian (wind-blown) bedforms using the Shuttle Radar Topography Mission (SRTM) digital elevation data Remote Sensing of Environment 100,179-189.

Breed, C.S., Grow, T., 1979. Chapter J. Morphology and distribution of dunes in sand seas observed by remote sensing, in: McKee, E.D. (Eds.), A Study of Global Sand Seas. U.S Geological Survey, Washington, pp. 253-302.

Breed, C.S., Fryberger, S.G., Andrews, S., McCauley, C., Lennartz, F., Gebel, D. and Horstman, K.,1979. Chapter K. Regional studies of sand seas, using land sat (ERTS) imagery, in: McKee, E.D. (Eds.), A Study of Global Sand Seas. U. S. Geological Survey, Washington, pp. 305-397.

Brown, G.F., 1960. Geomorphology of western and central Saudi Arabia. 21st International geological Congress, Copenhagen, 150-159.

Brown, G.F., Layne, N., Goudarzi, G.H., MacLean, W.H., 1963. Geologic map of the northeastern Hijaz quadrangle, Kingdom of Saudi Arabia: US Geological Survey Misc. Geol. Inv. Map I-205A.

Bullard, J.E., White, K., Livingstone, I., 2011. Morphometric analysis of aeolian bedforms in the Namib Sand Sea using ASTER data. Earth Surface Processes and Landforms 36, 1534-1549.

Bunker, D.G., 1953. The southwest borderlands of the Rub Al-Khali. Geological Journal119, 420-430.

Burckhardt, J.L., 1829. Travels in Arabia . Henry Colburn, London.

Clark, A., 1989. Lakes of Rub Al- Khali . Aramco World 40, 28-33.

Cooke, R.U., Warren, A., Goudie, A.S., 1993. Desert Geomorphology, UCL Press, London. 526p.

Doughty, C.M., 1888. Travels in Arabia, Cambridge University press, London, 690p.

Edgell, H.S., 1989. Evolution of Rub' Al- Khali desert. Jour. King Abdul Aziz University, Earth Sciences, Special Issue, 1st Saudi Arabia Symposium on Earth Sciences, Jeddah Saudi Arabia, 109-126.

Edgell, H.S., 2006. Arabian Deserts: Nature, Origin and Evolution. Springer.

El-Sayed, M.I., 1999. Sedimentological characteristics and morphology of the aeolian sand dunes in the eastern part of the UAE: a case study from Ar Rub' Al- Khali. Sedimentary Geology 123, 219-238.

El-Sayed, M.I., 2000. The nature and possible origin of mega-dunes in Liwa, Ar Rub' Al- Khali. Sedimentary Geology 134, 305-330.

Ewing, R.C., Kocurek, G. 2010a. Aeolian dune-field pattern boundary conditions, Geomorphology 114, 175-187.

Ewing, R.C, Kocurek, G., 2010b. Aeolian dune interactions and dune field and dune field pattern formation: White Sand Dunefield, New Mexico, Sedimentology 57, 1119-1219.

Ewing, R.C., Kocurek, G., Lake, L.W., 2006. Pattern analysis of dune-field parameters. Earth Surface Process and Landforms 31, 1176-1191.

Fryberger, S.G., Ahlbrandt, T.S., 1979, Mechanisms for the formation of aeolian sand seas. Geomorphology 23, 440-460.

Fryberger, S.G., Dean, G., 1979. Dune forms and wind regime, in: McKee, E.D. (Eds.), A Study of Global Sand Seas. US Geological Survey, Washington, pp. 137-170.

Falorni, G., Teles, V., Vivoni, E.R., Bras,R.L., Amaratunga, K.S., 2005. Analysis and characterization of the vertical accuracy of digital elevation models from the Shuttle Radar Topography Mission, Journal of Geophysical Research 110, 1-20.

Glennie, K.W., 1970. Desert sedimentary environments, in: Glennie, K.W. (Eds.), Developments in Sedimentology 14, Elsevier, pp. 1-22.

Glennie, K.W., 1998. The desert of southeast Arabia: a product of Quaternary climatic change, in: Alsharhan, K.W., Whittle, G.L., Kendall, G.G. (Eds.), Quaternary Deserts and Climatic Change. Balkema, Rotterdam, pp. 315-325.

Glennie, K.W., 2005. The desert of southeast Arabia: Desert Environments and Sediments. Gulf Petrolink, Bahrain.

Glennie, K.W., Singhvi, A.K., 2002. Event stratigraphy, paleoenvironment and chronology of SE Arabian deserts. Quaternary Science Reviews 21, 853-869.

Goudie, A.S, Colls, A., Stokes, S., Parker, a., White, K., Al-Farraj, A., 2000. Latest Pleistocene and Holocene dune construction at the north-eastern edge of the Rub Al Khali, United Arab Emirates, Sedimentology 47, 1011-1021.

Holm, D.A., 1960. Desert geomorphology in the Arabian Peninsula. Science 132, 1369-1379.

Holm, D.A., 1968. Sand dunes, in: R.W. Fairbridge, (Eds.) The encyclopedia of geomorphology: New York, Reinhold Book Corp., pp. 973-979.

Hotta, S., Kubota, S., Katori, S. ,Horikawa, K., 1984. Sand transport by wind on wet sand surface. Coastal Engineering, 1265-1281.

Hugenholtz, C.H., Barchyn, T. E., 2010. Spatial analysis of sand dunes with a new global topographic dataset: new approaches and opportunities. Earth Surface Processes and Landforms 35, 986-992.

Hotzl, H., Kramer, F., Maurin, V., 1978. Quaternary sediments, in: Al-Sayari S.S, Zotel, J.G. (Eds.), Quaternary period in Saudi Arabia1. Springer-Verlag, Vienna, pp. 264-301.

Hunter, R.E, Richmond, B.M., Alpha, T.R., 1983. Storm-controlled oblique dunes of the Oregon Coast. Geological Society of America 94, 1450-1465.

Kocurek, G., 1998. Aeolian system response to external forcing- a sequence stratigraphic approach, in: Alsharhan, A.S., Glennie, K.W., Whittle, G.L., Kendall, G.G. (Eds.), Quaternary Desert and Climatic Change, Balkema, Rotterdam, pp. 327-338.

Kocurek, G., 1999. The aeolian rock record, in: Goudie, A.S., Livingstone, I., Stokes, S. (Eds.), Aeolian Environments Sediments and Landforms, Chichester, John Wiley and Sons Ltd, pp. 239-259.

Kocurek, G., Ewing, R.C., 2005. Aeolian dune field self-organization implication for the formation of simple versus complex dune-field patterns. Geomorphology 72, 94-105.

Kocurek, G., Fielder, G., 1982. Adhesion structures. Journal of Sedimentary Petrology 52, 1229-1241.

Kocurek, G., Havholm, K.G., 1993. Eolian sequence stratigraphy - a conceptual framework, in: Weimer, P., Posamentier, H.W. (Eds.), Siciliclastic Sequence Stratigraphy. American Association of Petroleum Geologist Memoir 58, pp.393-409.

Kocurek, G., Lancaster, N., 1999. Aeolian system sediment state: theory and Mojave Desert Kelso dune field example. Sedimentology 46, 505-515.

Kocurek, G., Ewing, R.C., Mohrig, D., 2010. How do bedform patterns arise? New views on the role of bedform interactions within a set of boundary conditions. Earth Surface and Landforms 35, 51-63.

Kumar, A., Mahmoud, M.A., 2011. An overview of Origin, Morphology and Distribution of Desert Forms, Sabkhas and Playas of the Rub' Al- Khali Desert of the Southern Arabian Peninsula, Earth Science India 4, 105-135.

Lancaster, N., 1983. Controls of dune morphology in the Namib Sand Sea, in: Brookfield, M. E., Ahlbrandt, T. S., (Eds.), Eolian Sediments and processes, Amesterdam: Elseiver, pp. 261-89.

Lancaster, N., 1988. Controls of eolian dune size and spacing, Geology 16, 972-975.

Lancaster, N., 1989. The Namib sand sea- dune forms, processes and sediments. Rotterdam: Balkema. 200.

Lancaster, N., 1994. Controls on aeolian activity: some new perspective from the Kelso Dunes, Mojave Desert, California, Journal of Arid Environment 27, 113-125.

Lancaster, N., 1998. Dune Morphology, Chronology and Quaternary climatic changes, in: Alsharhan, K. W., Whittle, G. I., Kendall, G.G. (Eds.), Quaternary Deserts and climate Change. Balkema, Rotterdam, pp. 339-349.

Lancaster, N., Tchakerian, V.P., 2003. Late Quaternary eolian dynamics, Mojave Desert, California, in: Enzel, Y., Wells, S. G., Lancaster, N. (Eds.), Paleoenvironments and Paleohydrology of the Mojave and Southern Great Basin Deserts. Geological Society of America, pp. 231–249.

Laity, J., 2009. Desert and Desert Environments.. John Wiley and Sons, 360 p.

Livingstone I., Warren A., 1996. Aeolian geomorphology. Addison Wesley Longman Limited.

McClure, H.A., 1976. Radiocarbon chronology of the Late Quaternary Lakes in the Arabian Desert. Nature 263, 755-756.

McClure, H.A., 1978. Ar Rub' Al- Khali, in: Al-sayari, S.S., Zölt, J.G. (Eds.), Quaternary Period in Saudi Arabia, Springer-Verlag, Vienna, pp. 252-263.

Mckee, E.D., 1979. Introduction to a study of global sand sea, in: McKee, E.D. (Eds.), A Study of Global Sand Seas. U. S. Geological Survey Washington, pp.1-19.

McKee, E.D. Bigarella, J., 1979. Sedimentary structures in dunes, in: McKee, E. D. (Eds.), A Study of Global Sand Seas. U. S. Geological Survey, Washington, pp. 83-134.

McKee, E.D., Breed, C.S., 1976. Sand seas of the world, in: Williams, R.S, Carter, W. D. (Eds.) ERTS-1, A new window on our planet. US Geological Survey, pp. 81-88.

Membery, D.A., 1983. Low-level wind profiles during the Gulf Shamal. Weather 38, 18– 24.

Mountney, N.P., 2006. Periodic accumulation and destruction of aeolian erg sequences: The Cedar Mesa Sandstone, White Canyon, southern Utah. Sedimentology 53, 789-823.

Mountney, N.P., 2012. A stratigraphic model to account for complexity in aeolian dune and interdune successions. Sedimentology 59, 964-989.

Mountney, N.P. and Russell, A.J., 2006. Coastal aeolian dune-field development and response to periodic fluvial inundation, Sólheimasandur, southern Iceland. Sedimentary Geology 192, 167-181.

Mountney, N.P. and Russell, A.J., 2009. Aeolian dune field development in a water table-controlled system: Skeiđarársandur, southern Iceland. Sedimentology 56, 2107-2131.

Mountney, N.P and Thompson, D.B., 2002. Stratigraphic evolution and preservation of aeolian dune and damp/wet interdune strata: an example from the

Triassic Helsby Sandstone Formation, Cheshire Basin, UK. Sedimentology 49, 805-834.

Olsen, H., Due, P.H., Clemmensen, L.B., 1989. Morphology and genesis of asymmetric adhesion warts- a new adhesion surface structure: Sedimentary Geology 61, 277-285.

Powers, R.W., Ramirez, C.D., Redmond, C.D., Elberg Jr., E.L., 1966. Geology of the Arab Peninsula: Sedimentary Geology of Saudi Arabia. U.S Geological Survey, Professional Paper 560-DUS, Washington, pp.1-147.

Preusser, F., 2009. Chronology of the impact of Quaternary climate change on continental environments in the Arabian Peninsula. Comptes Rendus Geoscience 341, 621-632.

Preusser, F., Radies, D., Matter, A., 2002. A 160,000-year record of dune development and atmospheric circulation in Southern Arabia. Science 296, 2018-2020.

Pye, K., Tsoar, H., 2009. Aeolian Sand and Sand Dunes, Springer, 458 p.

Rubin, D.M., 1987. Cross-bedding, bedforms and palaeocurrents. Society of Economic Paleontologists and Mineralogists Concepts in Sedimentology and Paleontology 1, 187 p.

Rubin, D.M., Carter C.L., 2006. Bedforms and Cross-Bedding in Animation, SEPM, Atlas 2, DVD.

Sarnthein, M., 1978. Sand desert during glacial maximum and climatic optimum. Nature 272, 43-46.

Sweet, M.L., Nielson, J., Havholm, K., Farrelly, J., 1988. Algodones dunefield of SE California: case history of a migrating modern dune field. Sedimentology 35, 939-952.

Thesiger, W., 1949. A further journey across the Empty Quarter. Geographical Journal 113, 21-46.

Warren, A., Knott, P., 1983. Desert Dunes: a Short Review of the Needs in Desert Dune Research and a Recent Study of Micro-Meteorological Dune-Initiation Mechanisms, in Brookfleld, M.E., Ahlbrandt, T.S. (Eds). Eoilan Sediments and Processes Developments, Sedimentology 38, pp. 343-352.

Werner, B.T., Kocurek, G., 1997. Bed-form dynamics: dose the tail wag the dog. Geology 25, 771-774.

Wilkins, D.E., Ford, R.L., 2007. Nearest neighbour methods applied to dune field organization: the Coral Pink Sand Dunes, Kane County, Utah, USA. Geomorphology 83, 48-57.

Wilson, I.G., 1972. Aeolian bedforms – Their development and origins: Sedimentology 19, 173-210.

Wilson, I.G., 1973. Ergs, Sedimentary Geology 10, 77-106.

Table and Figure Captions

Table 1: Summary of data relating to geometry of 555 dunes in the studied part of the Rub' Al-Khali sand sea.

Table 2: Summary of data relating to geometry of 1415 interdunes in the studied part of the Rub' Al-Khali sand sea.

Figure 1: (a) Map of the Arabian Peninsula showing the location of the Rub' Al-Khali sand sea, dune-fields within which are the focus of this study.. Image from Google Earth Pro. (b) Map of Arabian Peninsula outlining geomorphological referred to in the text. Modified after Edgell (2006). Location of area of detailed study shown in figure 2a is indicated.

Figure 2: (a) Map of part of south-eastern Saudi Arabia showing the location of the areas named 1, 2, 3, and 4 for this study. Location of regions shown in figures 2b and 2c are indicated. Letters A-D refer to the location of the images shown in figure 5. Lines A-A' to J-J' are transects across different

parts of the study areas and are shown in figures 6 and 7. (b) Satellite images from the study area depicting the typical geomorphology of the dune fields, and the variation in dune morphology and distribution from the central part of the dune fields toward their margins. Note the reduction in dune size in a direction toward the dune-field margins, and the concomitant increase in the extent and connectivity of interdunes and playa areas. Images from Google Earth Pro.

Figure 3: Maps of the study areas depicting the locations from which quantitative data regarding dune and interdune morphology and geometry were collected. (a) Location of transects from which data relating to interdune morphology were collected. (b) Location of transects from which data relating to dune morphology were collected; transects relate to areas 1-4 and also to a north-south line (NS). See supplementary data entries 1 and 2 for detailed information regarding sites of data collection.

Figure 4: Example of dunes and interdunes of the Rub' Al-Khali, including definitions of the terminology used in this study to quantitatively describe their morphology and geometry. (a) Satellite imagery showing plan-form morphology. (b) Cross-sections derived from DEM data. (c) Schematic illustration of how bedform spacing has been determined for different morphological bedform types. Measurements made using Google Earth Pro software; data are recorded in a relational database, which has been queried to determine common trends and determine styles of spatial change in geometry and morphology across the study region.

Figure 5: A summary of dominant wind directions for the central and eastern part of the Rub' Al-Khali, based on data from 1982 to 2013 collected from 5 stations. Values in table are in percent. See Figure 1a for location of stations. Source: WeatherOnline.

Figure 6: Satellite images from different locations across the Rub' Al-Khali desert depicting typical variations in dune and interdune morphology. Note the contrast in dune form and size between each image. All images depicted at the same scale. See figure 2a for locations. (a) Image from the northern

part of Study Area 1, north-eastern Rub' Al-Khali, showing rows of laterally linked mega-barchan dunes with intervening interdunes (salt flats). (b) Image from the northern part of Study Area 2, north Rub' Al-Khali, showing a region dominated by complex giant barchan dunes with superimposed crescentic dune forms and parallel interdune corridors. (c) Image from the southern part of Study Area 3, southeast Rub' Al-Khali, showing an example of compound linear dune ridges, each separated by wide and parallel interdune corridors. (d) Image from the central part of Study Area 4, southeast Rub' Al-Khali, depicting an area characterized by pyramidal dunes (star bedforms) with distinctive star-like plan-form shapes and surrounded by extensive interdune areas.

Figure 7: Cross sections from study areas 1-4 with elevation data reflecting variation in dune and interdune morphology and spacing from the centre of the dune field to its margin. The location of the cross sections is shown in Figure 2a. Digital Elevation data from Google Earth Pro are accurate to +/- 10 m.

Figure 8: Cross sections from different positions in the study areas 1-4 with elevation data reflecting variation in dune and interdune morphology and spacing. The location of the cross sections is shown in Figure 2a. Sections E-E', F-F', G-G' and H-H' are aligned close to parallel to the regional resultant drift direction (toward the southeast); Section I-I' is aligned close to perpendicular to the regional resultant drift direction across a series of linear bedforms. Section J-J' reveals spatial changes in the morphology and geometry of star bedforms in the southern part of the study area. Digital Elevation data from Google Earth Pro are accurate to 10 m. Note that the dune wavelengths and interdune widths depicted in the cross sections are apparent since the orientation of the bedforms is oblique to the regional resultant drift direction in most cases.

Figure 9: Examples of data demonstrating relationships present in aspects of dune bedform morphology in the Rub' Al-Khali dune field, showing the relationship between different parameters measured in the study area. Dune heights record the relief change between bedform crests and the

generalised level of the desert floor as defined by the level of interdune flats in marginal areas of the dune fields. Best-fit lines shown on graph are for all data; separate best-fit equations are additionally shown for individual data sets from each study area. See text for further explanation.

Figure 10: Examples of data demonstrating relationships present in aspects of dune bedform height and interdune elevation in the Rub' Al-Khali dune field, showing the relationship between different parameters measured in the study area. Best-fit lines shown on graph are for all data; separate best-fit equations are additionally shown for individual data sets from each study area. Dune heights have been calculated based on relief above the regional level of the desert floor in the dune-field margin areas; note that this level is higher in Area 4 where the desert system is constructed on a slightly elevated basement, as shown in graph d. See text for further explanation.

Figure 11: Examples of data demonstrating relationships present in aspects of interdunes of the Rub' Al-Khali dune field. The scatter plots demonstrate several relationships between measured interdune parameters. Best-fit lines shown on graph are for all data; separate best-fit equations are additionally shown for individual data sets from each study area. See text for further explanation.

Supplementary data 1: Map depicting locations from where measurements of interdune geometry and morphology were made.

Supplementary data 2: Map depicting locations from where measurements of dune geometry and morphology were made.

Supplementary data 3. Relationship between cross sections E-E', F-F', G-G', H-H' and I-I' (shown in figure 7) to planform dune and interdune morphology as revealed by Google Earth Pro imaging.

Table 01

Table 1 - Dune data summary

Dune measured parameters \ Statistical analysis	Minimum	Maximum	Mean	Standard Deviation	Coefficient of Variance
Amplitude of along-crest sinuosity (km)	0.03	2.39	0.69	0.52	75.23
Wavelength of along-crest sinuosity (km)	0.11	4.99	2.02	1.17	57.89
Minimum wavelength (km)	0.01	2.04	0.52	0.40	78.18
Maximum wavelength (km)	0.05	3.34	1.22	0.72	58.89
Spacing (km)	0.63	8.41	3.05	1.21	39.78
Height (m)	67	218	144.42	31.49	21.80

Table 02

Table 2: Interdune data summary

Interdune measured parameters \ Statistical analysis	Minimum	Maximum	Mean (km)	Standard Deviation	Coefficient of Variance
Length (km)	0.20	53.15	6.97	8.19	117.54
Width (km)	0.06	6.22	1.49	0.88	58.95
Orientation (degrees)	5	221	106.39	35.63	33.49
Elevation (m)	60	107	76.17	9.96	13.08

Figure 01a


a
Iraq
Iran
West Bank
Gaza Strip
Israel
Jordan
Kuwait
Bahrain
Qatar
Al-Hasa
Riyadh
Saudi Arabia
United Arab Emirates
Figure 2a
Rub' Al-Khali sand sea
Oman
Wadi
Ad-Dawaser
Najran
Sharurah
Yemen
N
0
km
500

Figure 01b

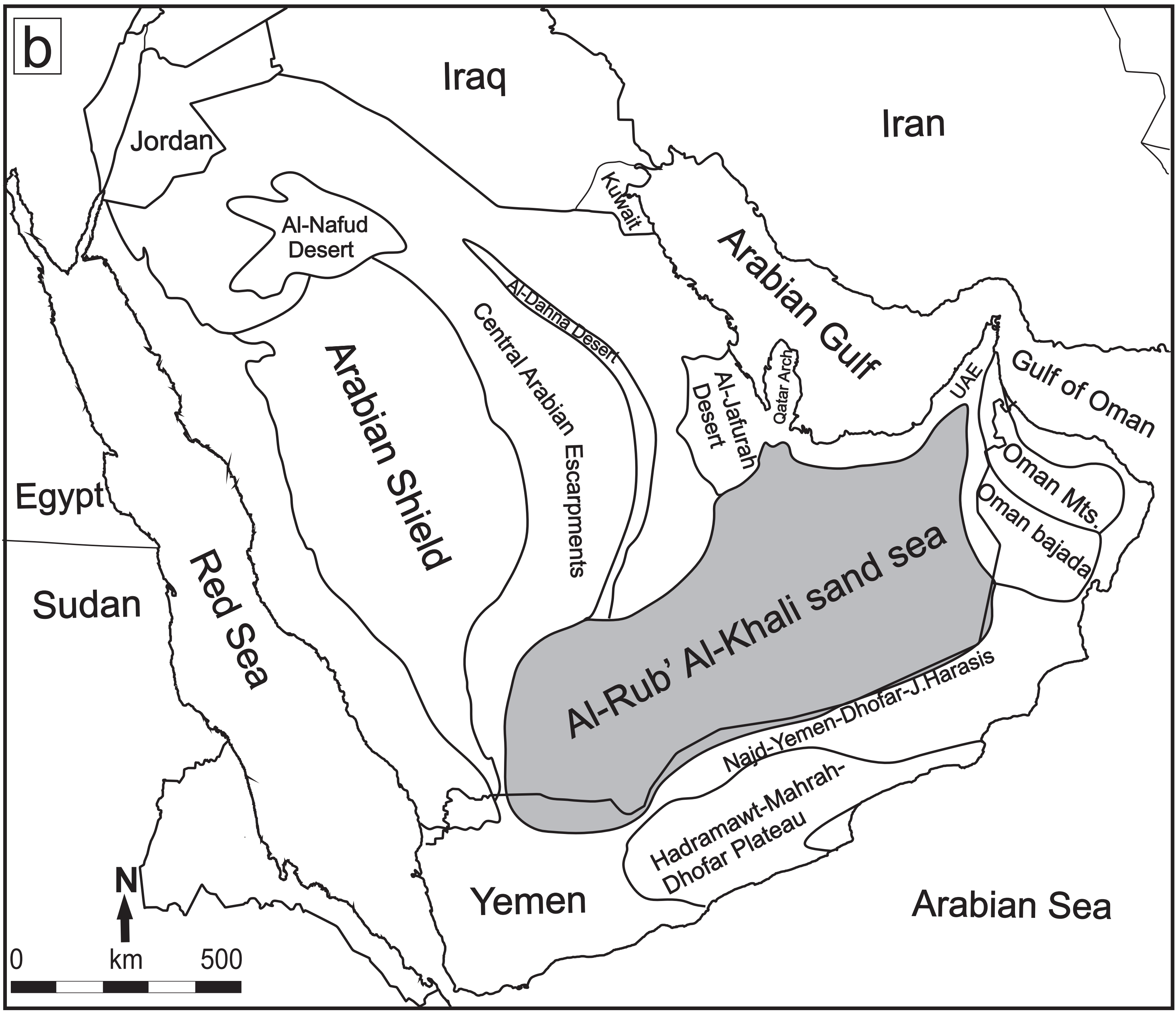
b
Iraq
Iran
Jordan
Kuwait
Al-Nafud Desert
Arabian Gulf
Al-Dahna Desert
Central Arabian Escarpments
Arabian Shield
Al-Jafurah Desert
Qatar Arch
UAE
Gulf of Oman
Oman Mts.
Oman bajada
Egypt
Sudan
Red Sea
Al-Rub' Al-Khali sand sea
Najd-Yemen-Dhofar-J.Harasis
Hadramawt-Mahrah-Dhofar Plateau
Yemen
Arabian Sea
N
0
km
500

Figure 02a

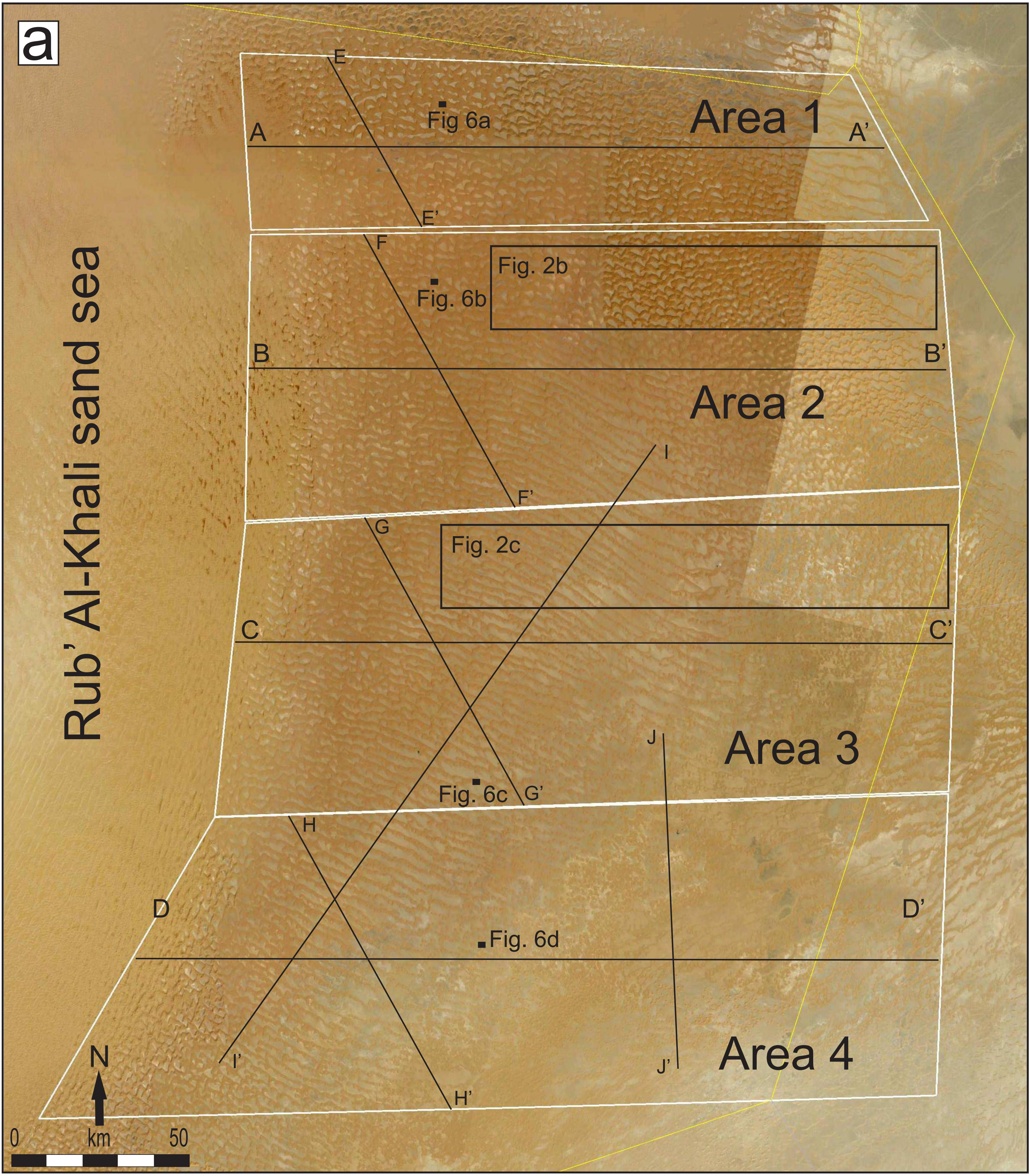
a
Rub' Al-Khali sand sea
Area 1
Area 2
Area 3
Area 4
A
A'
B
B'
C
C'
D
D'
E
E'
F
F'
G
G'
H
H'
I
I'
J
J'
Fig 6a
Fig. 6b
Fig. 6c
Fig. 6d
Fig. 2b
Fig. 2c
N
0
km
50

Figure 2b and c

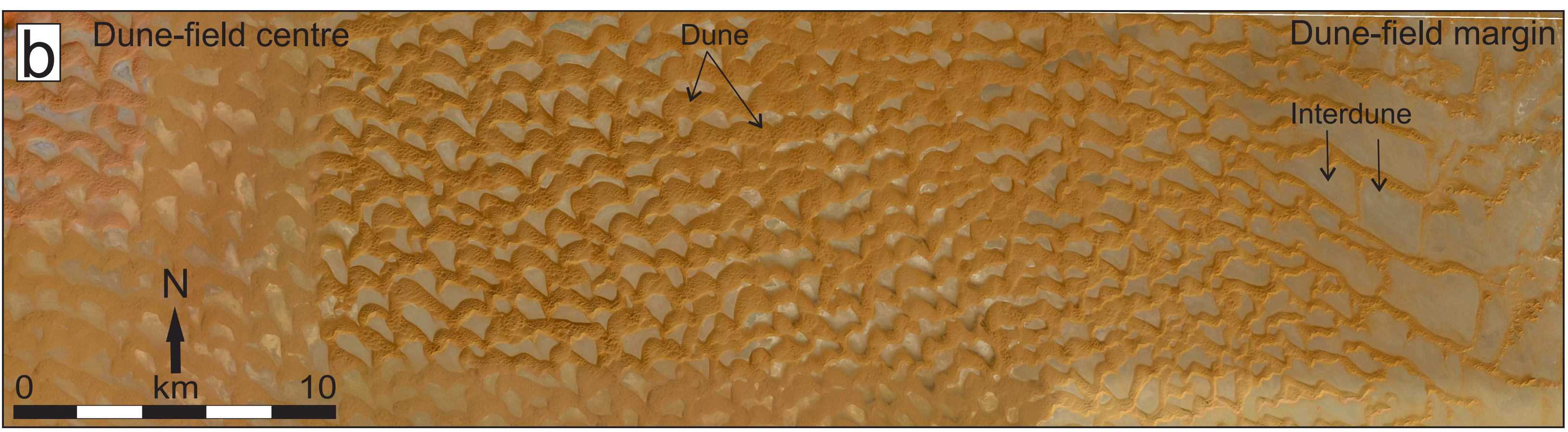

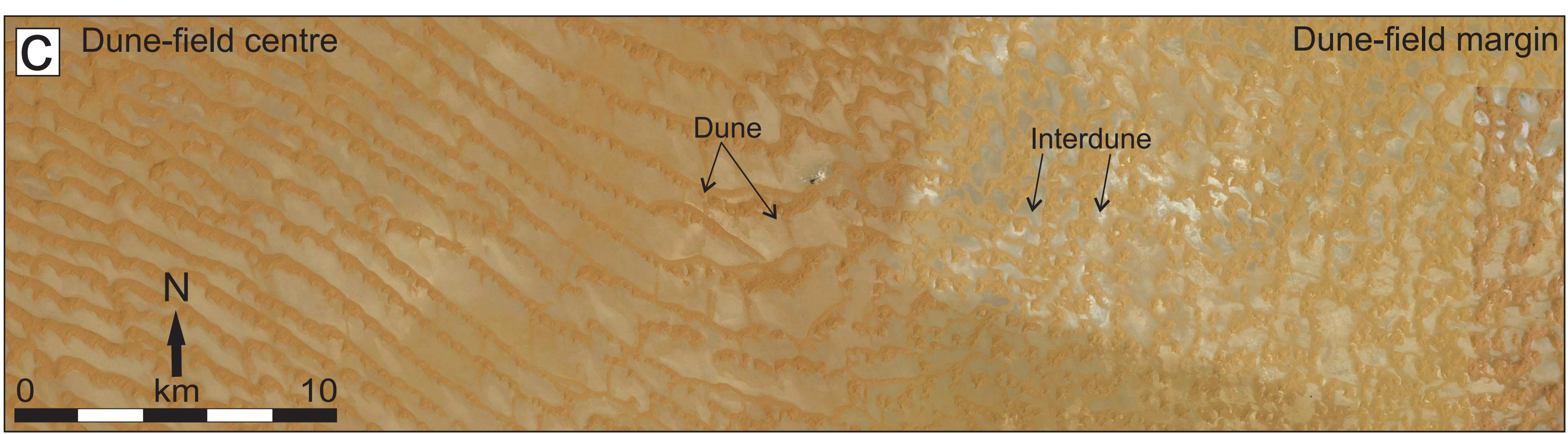

Figure 03

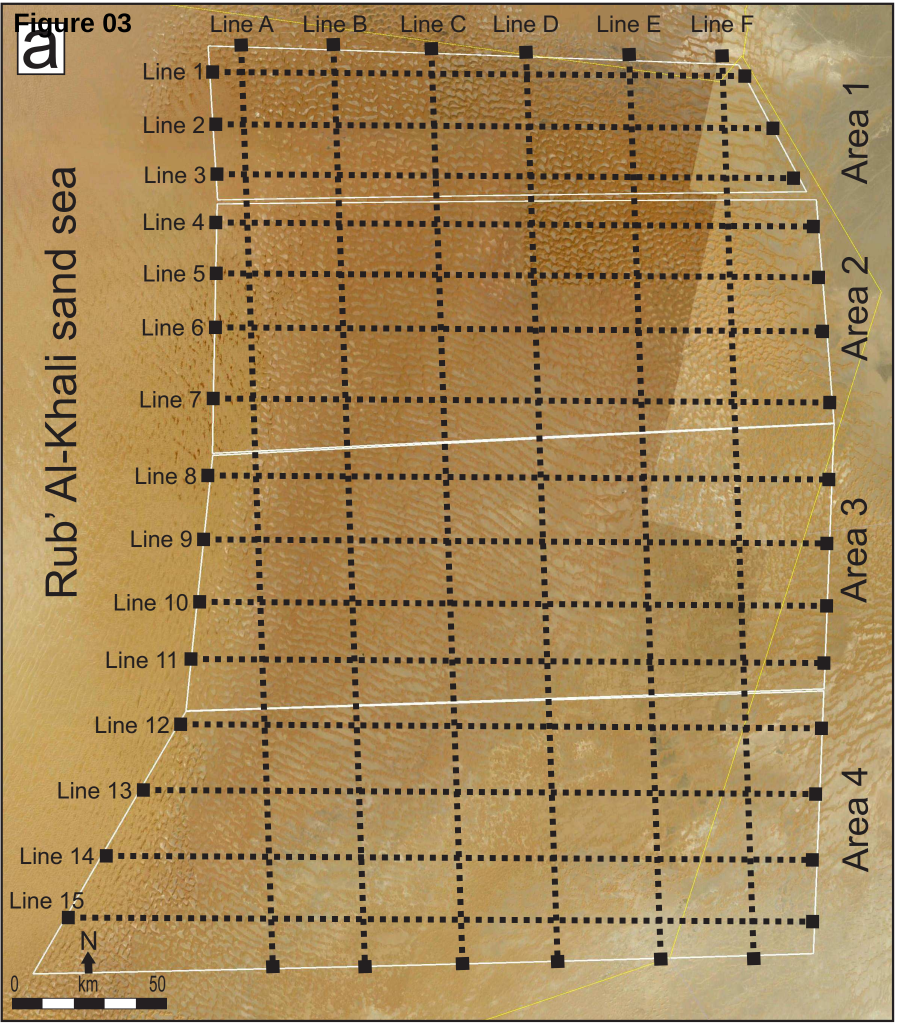
a
Line A
Line B
Line C
Line D
Line E
Line F
Line 1
Line 2
Line 3
Line 4
Line 5
Line 6
Line 7
Line 8
Line 9
Line 10
Line 11
Line 12
Line 13
Line 14
Line 15
Area 1
Area 2
Area 3
Area 4
Rub' Al-Khali sand sea
N
0
km
50

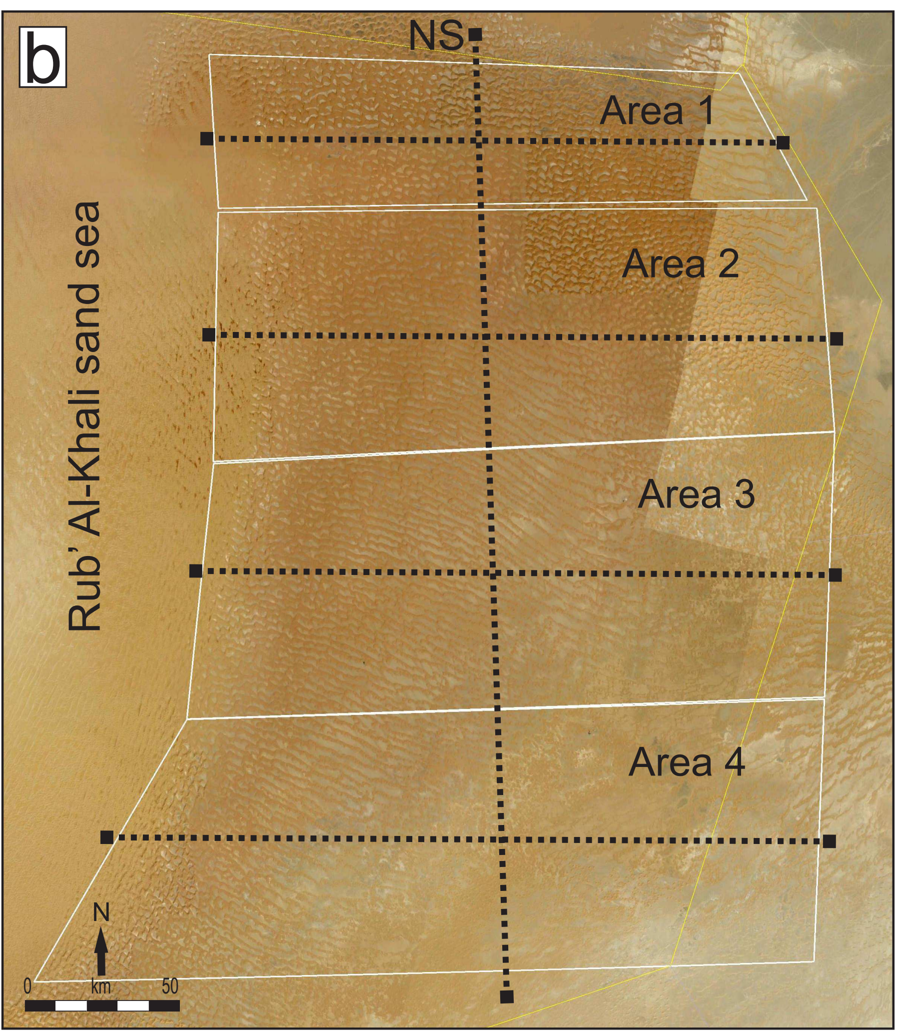
b
NS
Area 1
Area 2
Area 3
Area 4
Rub' Al-Khali sand sea
N
0
km
50

Figure 04

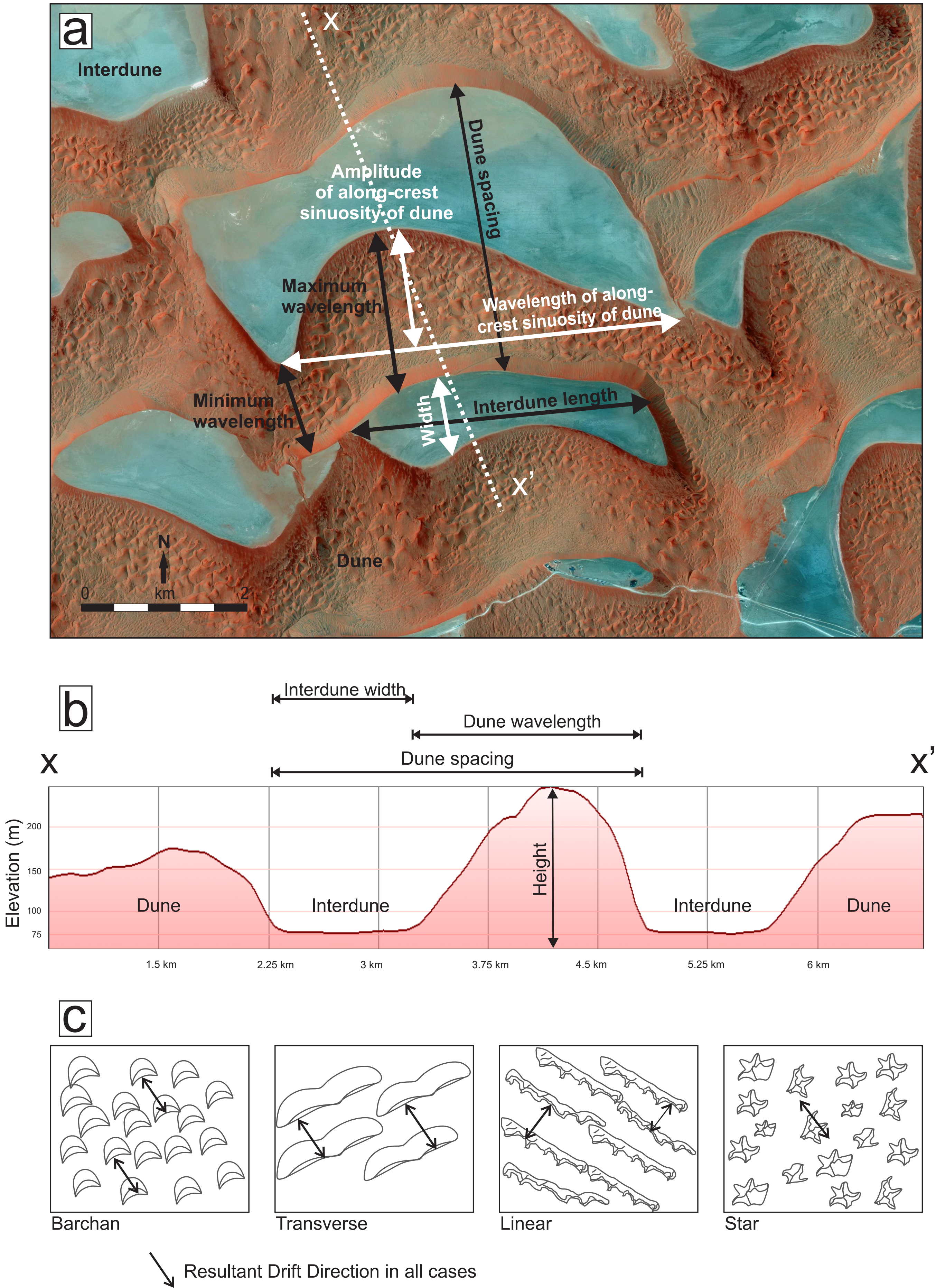

a
X
Interdune
Amplitude
of along-crest
sinuosity of dune
Dune spacing
Maximum
wavelength
Wavelength of along-
crest sinuosity of dune
Minimum
wavelength
Width
Interdune length
X'
N
0
km
2
Dune
b
Interdune width
Dune wavelength
Dune spacing
X
X'
Elevation (m)
200
150
100
75
Dune
Interdune
Height
Interdune
Dune
1.5 km
2.25 km
3 km
3.75 km
4.5 km
5.25 km
6 km
c
Barchan
Transverse
Linear
Star
Resultant Drift Direction in all cases

Figure 05

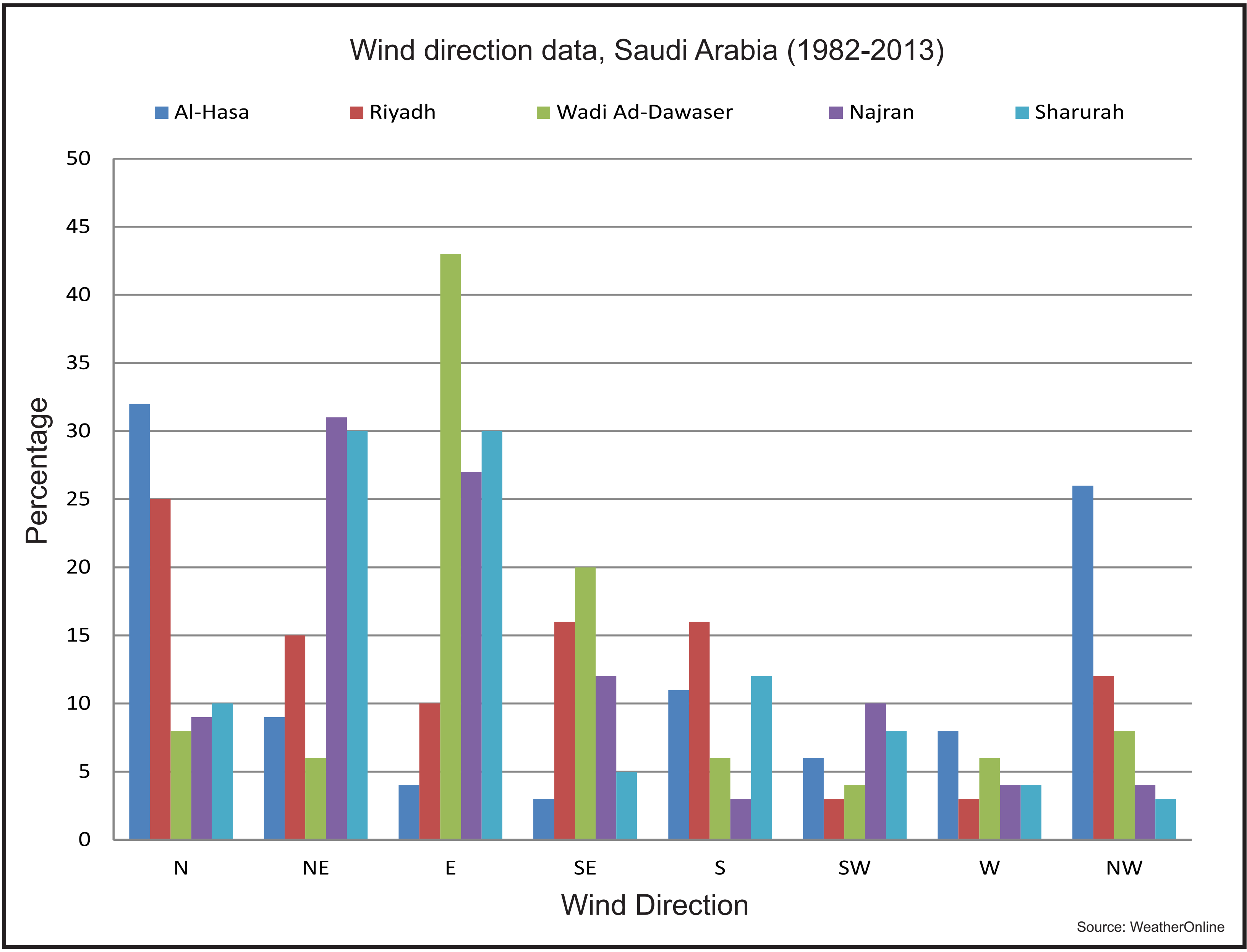

	Al-Hasa	Riyadh	Wadi Aldawaser	Najran	Sharurah
N	32	25	8	9	10
NE	9	15	6	31	30
E	4	10	43	27	30
SE	3	16	20	12	5
S	11	16	6	3	12
SW	6	3	4	10	8
W	8	3	6	4	4
NW	26	12	8	4	3

Figure 06

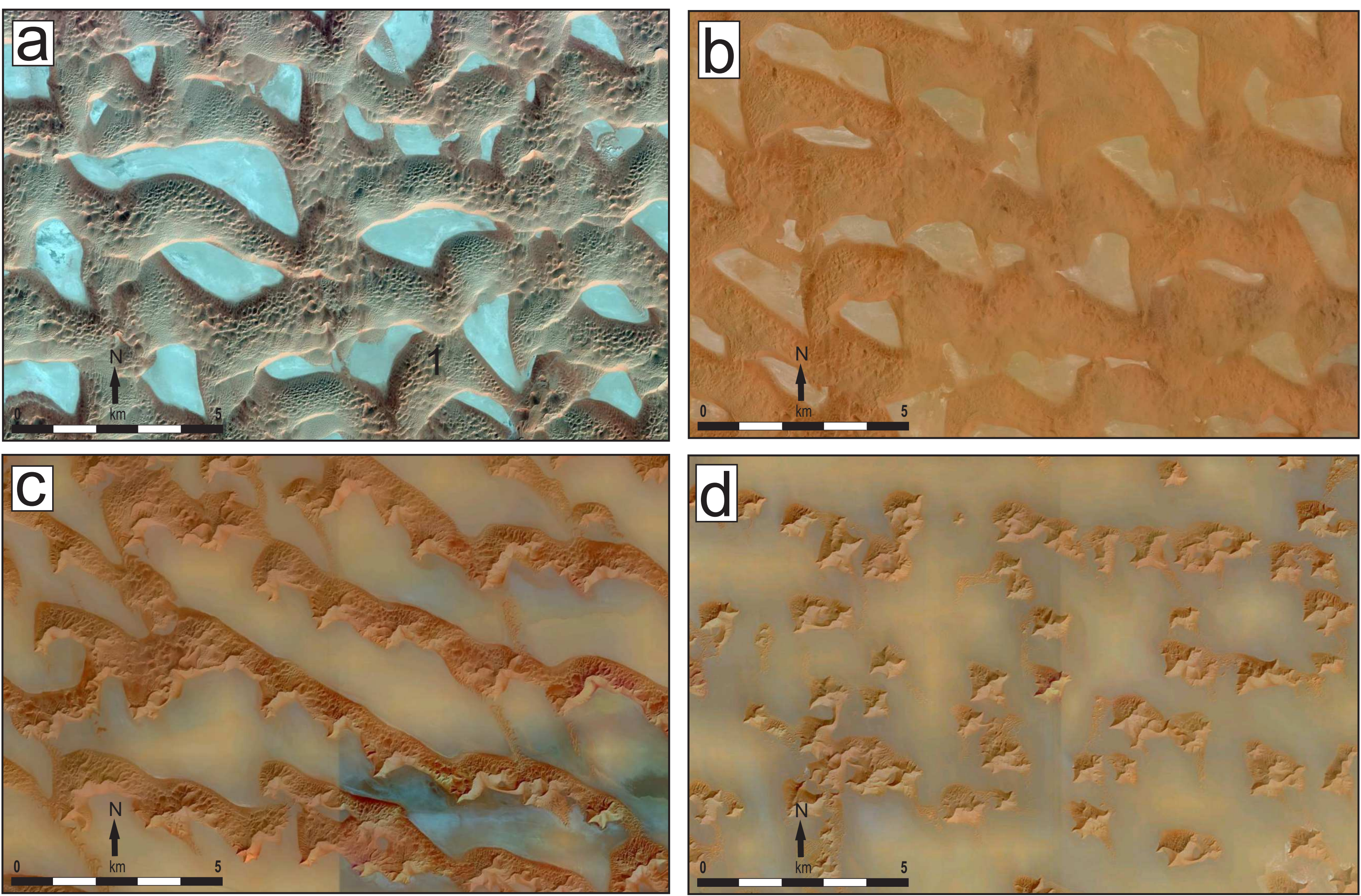

Figure 07

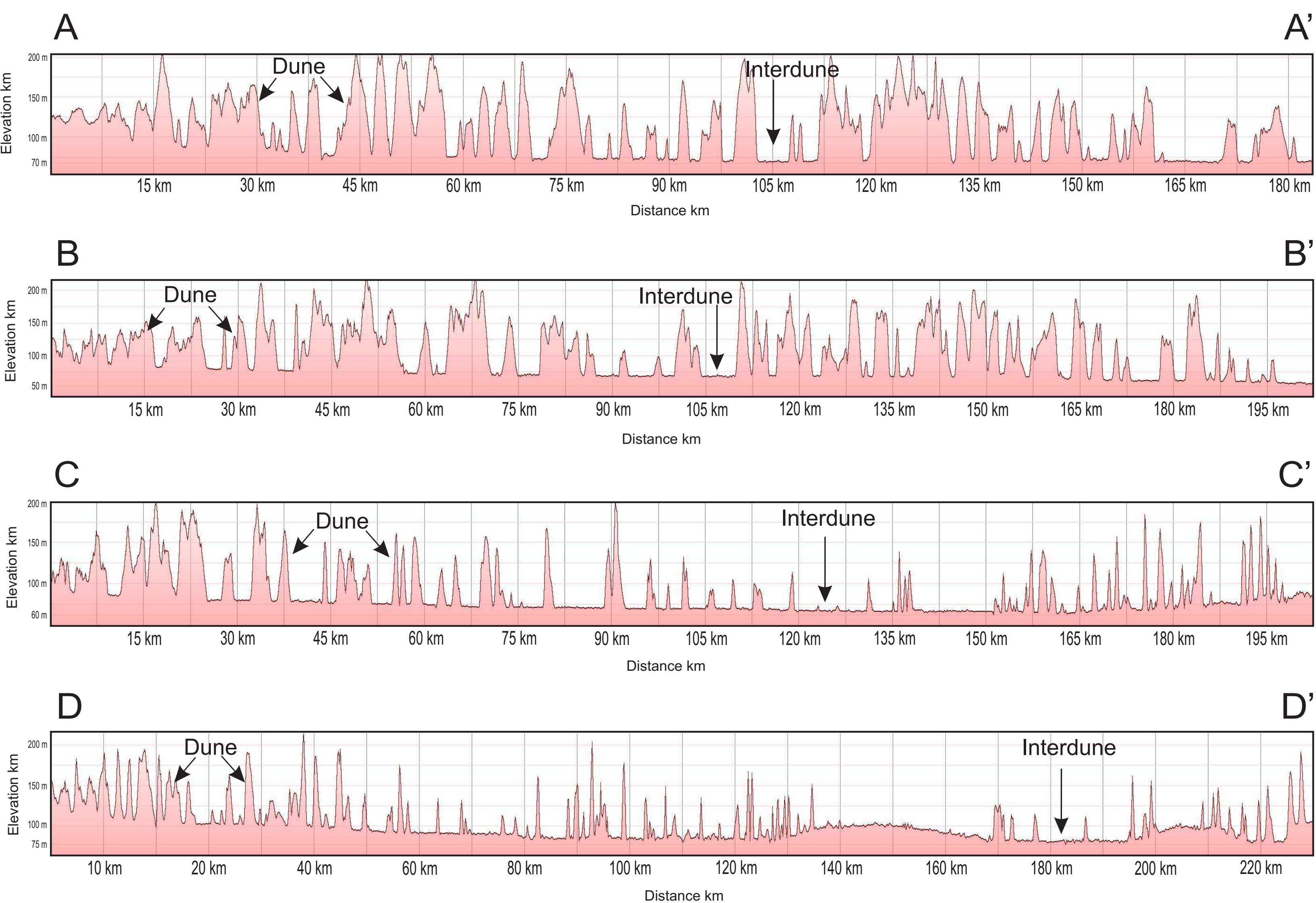
A
A'
Dune
Interdune
Elevation km
Distance km
B
B'
Dune
Interdune
Elevation km
Distance km
C
C'
Dune
Interdune
Elevation km
Distance km
D
D'
Dune
Interdune
Elevation km
Distance km

Figure 08

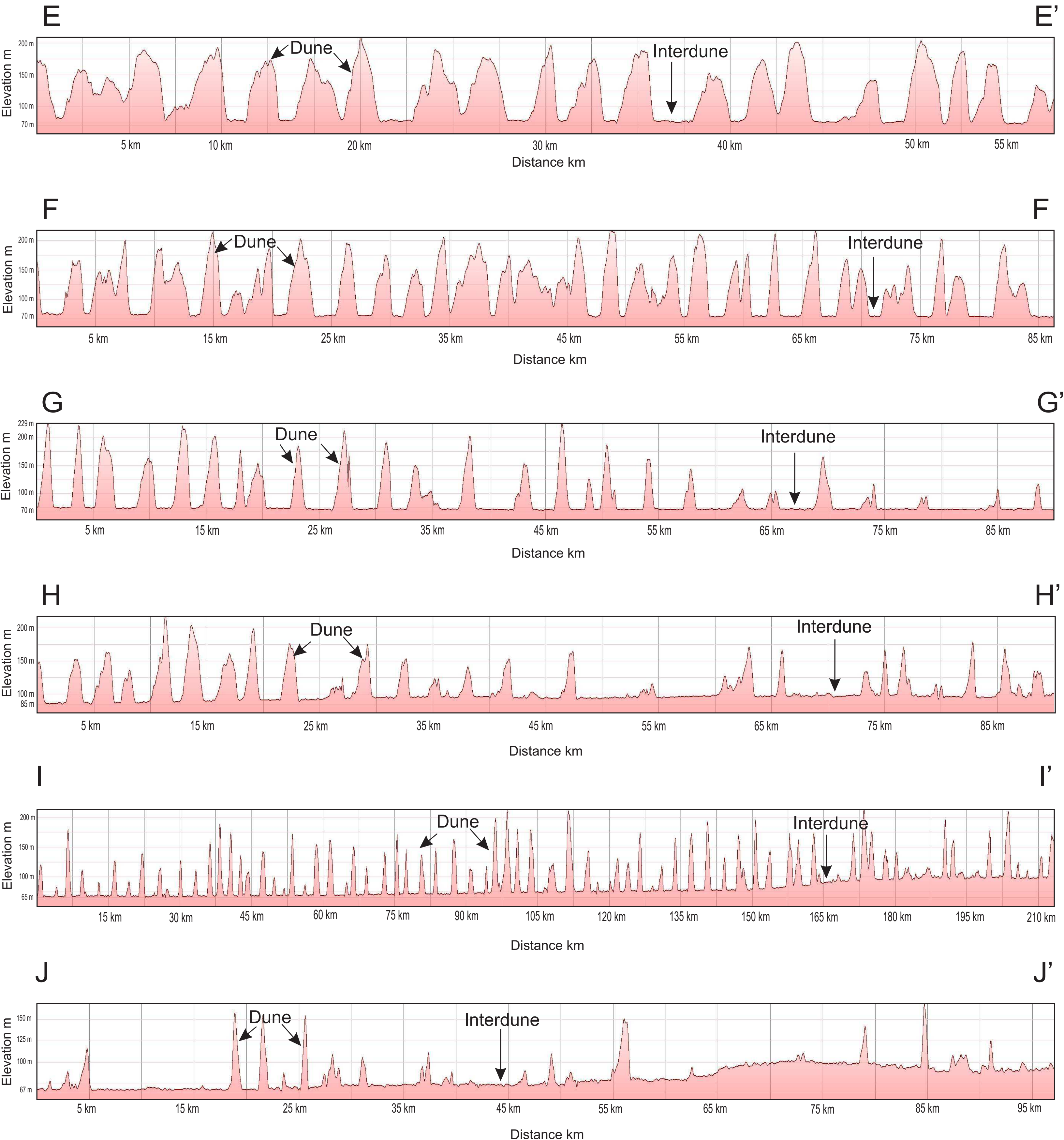

E
E’
Elevation m
200 m
150 m
100 m
70 m
Dune
Interdune
5 km
10 km
20 km
30 km
40 km
50 km
55 km
Distance km
F
F
Elevation m
200 m
150 m
100 m
70 m
Dune
Interdune
5 km
15 km
25 km
35 km
45 km
55 km
65 km
75 km
85 km
Distance km
G
G’
Elevation m
229 m
200 m
150 m
100 m
70 m
Dune
Interdune
5 km
15 km
25 km
35 km
45 km
55 km
65 km
75 km
85 km
Distance km
H
H’
Elevation m
200 m
150 m
100 m
85 m
Dune
Interdune
5 km
15 km
25 km
35 km
45 km
55 km
65 km
75 km
85 km
Distance km
I
I’
Elevation m
200 m
150 m
100 m
65 m
Dune
Interdune
15 km
30 km
45 km
60 km
75 km
90 km
105 km
120 km
135 km
150 km
165 km
180 km
195 km
210 km
Distance km
J
J’
Elevation m
150 m
125 m
100 m
67 m
Dune
Interdune
5 km
15 km
25 km
35 km
45 km
55 km
65 km
75 km
85 km
95 km
Distance km

Figure 09

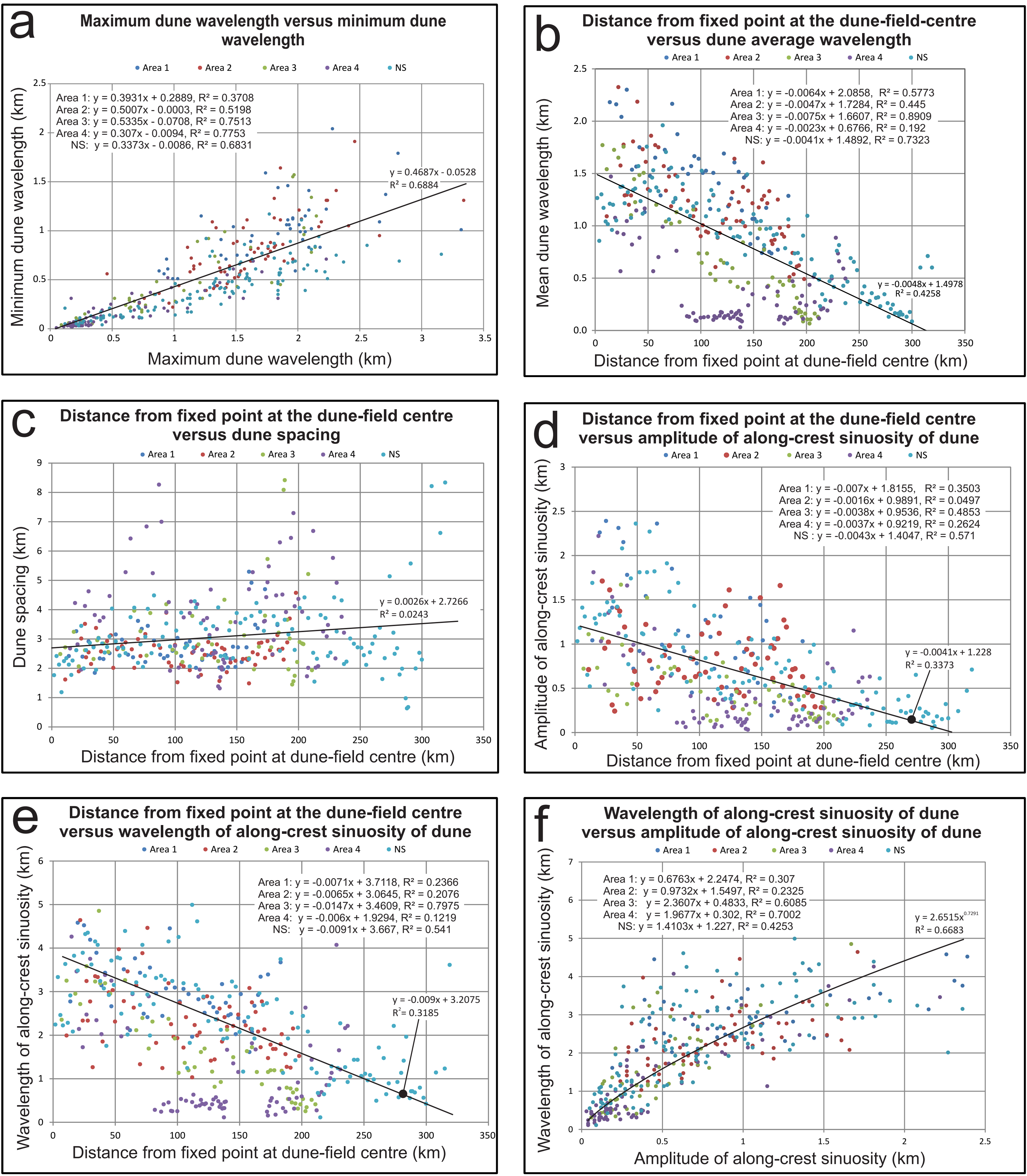
a
Maximum dune wavelength versus minimum dune wavelength
Area 1
Area 2
Area 3
Area 4
NS
Area 1: y = 0.3931x + 0.2889, R² = 0.3708
Area 2: y = 0.5007x - 0.0003, R² = 0.5198
Area 3: y = 0.5335x - 0.0708, R² = 0.7513
Area 4: y = 0.307x - 0.0094, R² = 0.7753
NS: y = 0.3373x - 0.0086, R² = 0.6831
y = 0.4687x - 0.0528
R² = 0.6884
Minimum dune wavelength (km)
Maximum dune wavelength (km)
b
Distance from fixed point at the dune-field-centre versus dune average wavelength
Area 1
Area 2
Area 3
Area 4
NS
Area 1: y = -0.0064x + 2.0858, R² = 0.5773
Area 2: y = -0.0047x + 1.7284, R² = 0.445
Area 3: y = -0.0075x + 1.6607, R² = 0.8909
Area 4: y = -0.0023x + 0.6766, R² = 0.192
NS: y = -0.0041x + 1.4892, R² = 0.7323
y = -0.0048x + 1.4978
R² = 0.4258
Mean dune wavelength (km)
Distance from fixed point at dune-field centre (km)
c
Distance from fixed point at the dune-field centre versus dune spacing
Area 1
Area 2
Area 3
Area 4
NS
y = 0.0026x + 2.7266
R² = 0.0243
Dune spacing (km)
Distance from fixed point at dune-field centre (km)
d
Distance from fixed point at the dune-field centre versus amplitude of along-crest sinuosity of dune
Area 1
Area 2
Area 3
Area 4
NS
Area 1: y = -0.007x + 1.8155, R² = 0.3503
Area 2: y = -0.0016x + 0.9891, R² = 0.0497
Area 3: y = -0.0038x + 0.9536, R² = 0.4853
Area 4: y = -0.0037x + 0.9219, R² = 0.2624
NS : y = -0.0043x + 1.4047, R² = 0.571
y = -0.0041x + 1.228
R² = 0.3373
Amplitude of along-crest sinuosity (km)
Distance from fixed point at dune-field centre (km)
e
Distance from fixed point at the dune-field centre versus wavelength of along-crest sinuosity of dune
Area 1
Area 2
Area 3
Area 4
NS
Area 1: y = -0.0071x + 3.7118, R² = 0.2366
Area 2: y = -0.0065x + 3.0645, R² = 0.2076
Area 3: y = -0.0147x + 3.4609, R² = 0.7975
Area 4: y = -0.006x + 1.9294, R² = 0.1219
NS: y = -0.0091x + 3.667, R² = 0.541
y = -0.009x + 3.2075
R² = 0.3185
Wavelength of along-crest sinuosity (km)
Distance from fixed point at dune-field centre (km)
f
Wavelength of along-crest sinuosity of dune versus amplitude of along-crest sinuosity of dune
Area 1
Area 2
Area 3
Area 4
NS
Area 1: y = 0.6763x + 2.2474, R² = 0.307
Area 2: y = 0.9732x + 1.5497, R² = 0.2325
Area 3: y = 2.3607x + 0.4833, R² = 0.6085
Area 4: y = 1.9677x + 0.302, R² = 0.7002
NS: y = 1.4103x + 1.227, R² = 0.4253
y = 2.6515x^0.7291
R² = 0.6683
Wavelength of along-crest sinuosity (km)
Amplitude of along-crest sinuosity (km)

Figure 10

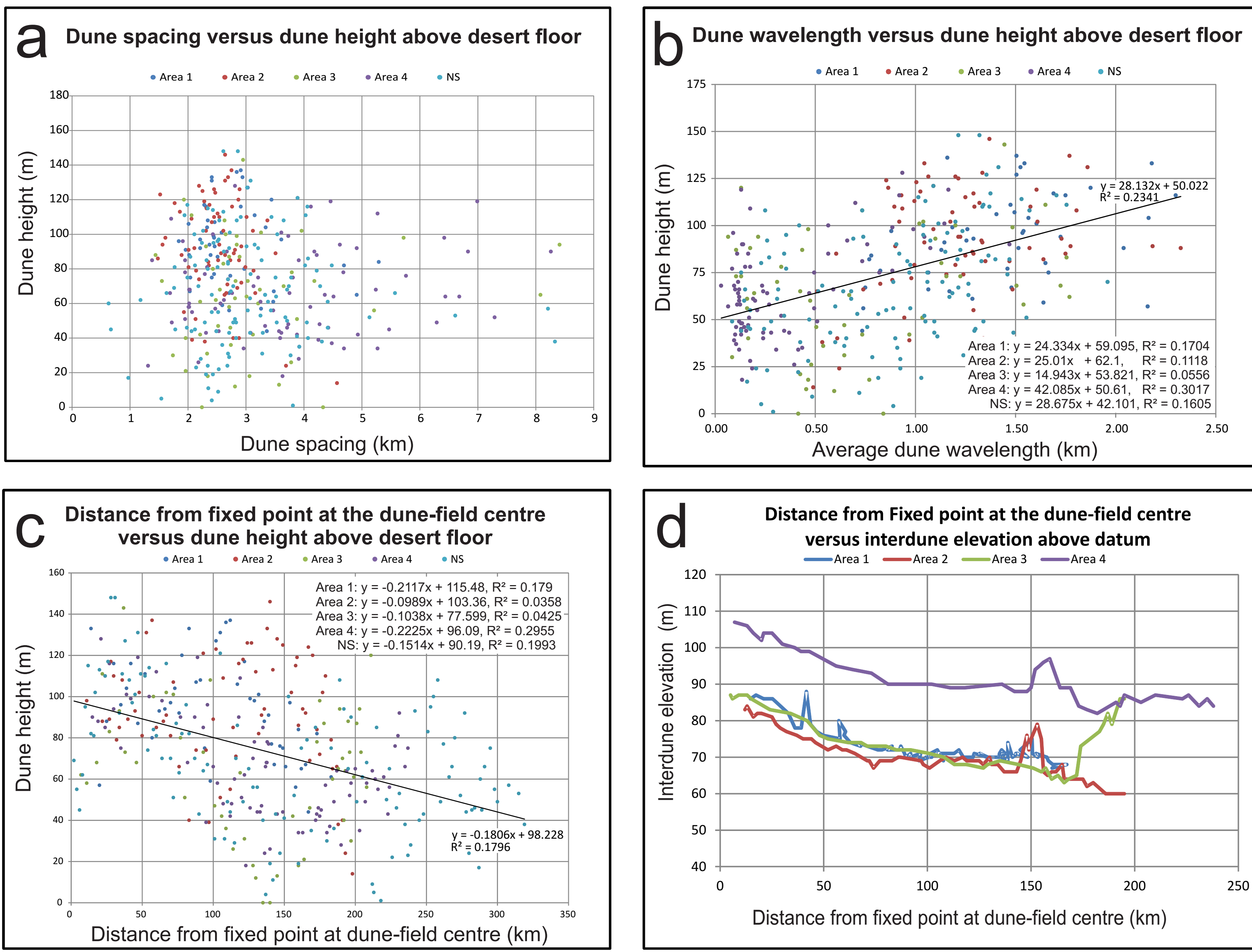
a
Dune spacing versus dune height above desert floor
Area 1 Area 2 Area 3 Area 4 NS
Dune height (m)
Dune spacing (km)
b
Dune wavelength versus dune height above desert floor
Area 1 Area 2 Area 3 Area 4 NS
y = 28.132x + 50.022
R² = 0.2341
Area 1: y = 24.334x + 59.095, R² = 0.1704
Area 2: y = 25.01x + 62.1, R² = 0.1118
Area 3: y = 14.943x + 53.821, R² = 0.0556
Area 4: y = 42.085x + 50.61, R² = 0.3017
NS: y = 28.675x + 42.101, R² = 0.1605
Dune height (m)
Average dune wavelength (km)
c
Distance from fixed point at the dune-field centre versus dune height above desert floor
Area 1 Area 2 Area 3 Area 4 NS
Area 1: y = -0.2117x + 115.48, R² = 0.179
Area 2: y = -0.0989x + 103.36, R² = 0.0358
Area 3: y = -0.1038x + 77.599, R² = 0.0425
Area 4: y = -0.2225x + 96.09, R² = 0.2955
NS: y = -0.1514x + 90.19, R² = 0.1993
y = -0.1806x + 98.228
R² = 0.1796
Dune height (m)
Distance from fixed point at dune-field centre (km)
d
Distance from Fixed point at the dune-field centre versus interdune elevation above datum
Area 1 Area 2 Area 3 Area 4
Interdune elevation (m)
Distance from fixed point at dune-field centre (km)

Figure 11

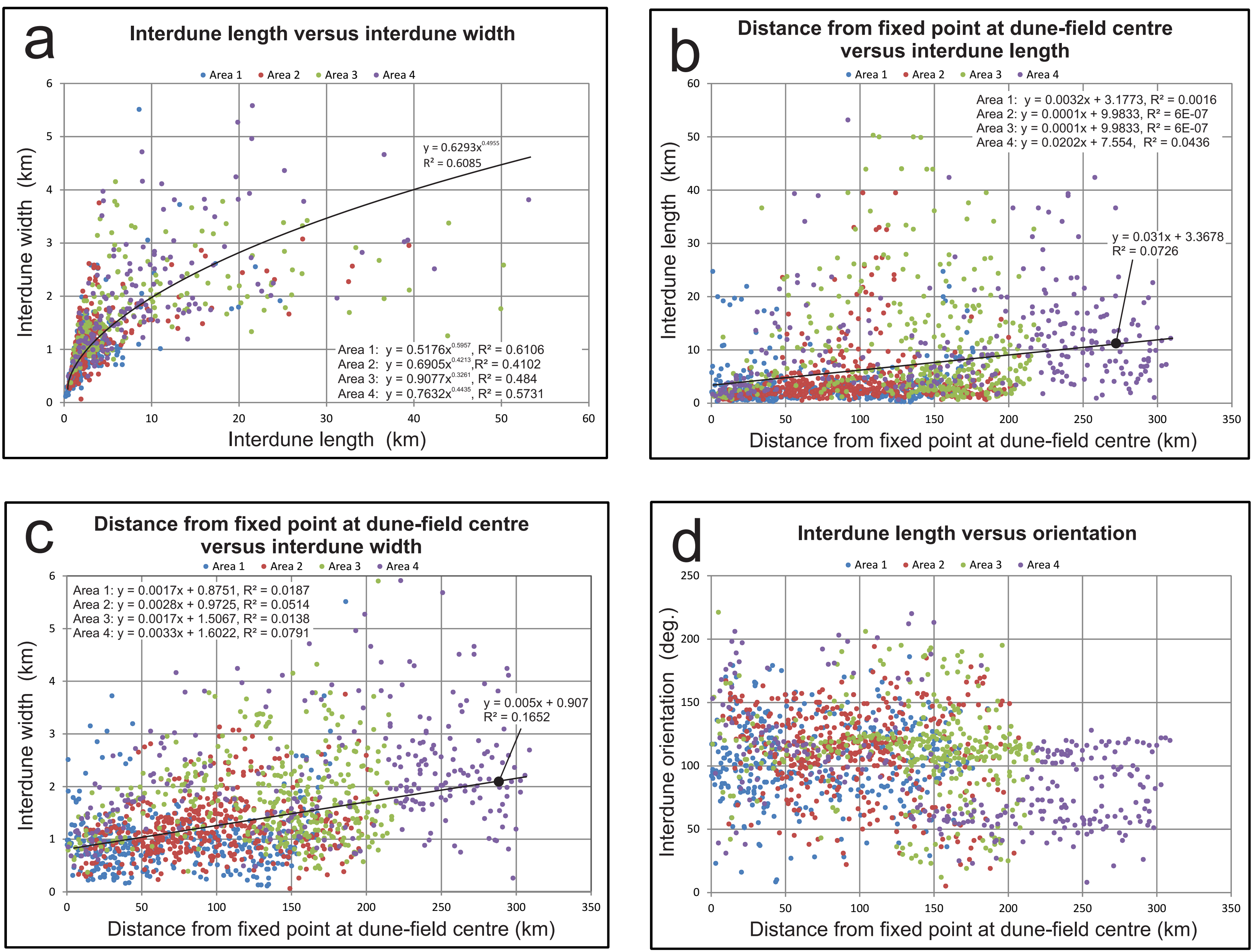
a
Interdune length versus interdune width
Area 1 Area 2 Area 3 Area 4
y = 0.6293x^0.4955
R² = 0.6085
Area 1: y = 0.5176x^0.5957, R² = 0.6106
Area 2: y = 0.6905x^0.4213, R² = 0.4102
Area 3: y = 0.9077x^0.3261, R² = 0.484
Area 4: y = 0.7632x^0.4435, R² = 0.5731
Interdune width (km)
Interdune length (km)
b
Distance from fixed point at dune-field centre versus interdune length
Area 1 Area 2 Area 3 Area 4
Area 1: y = 0.0032x + 3.1773, R² = 0.0016
Area 2: y = 0.0001x + 9.9833, R² = 6E-07
Area 3: y = 0.0001x + 9.9833, R² = 6E-07
Area 4: y = 0.0202x + 7.554, R² = 0.0436
y = 0.031x + 3.3678
R² = 0.0726
Interdune length (km)
Distance from fixed point at dune-field centre (km)
c
Distance from fixed point at dune-field centre versus interdune width
Area 1 Area 2 Area 3 Area 4
Area 1: y = 0.0017x + 0.8751, R² = 0.0187
Area 2: y = 0.0028x + 0.9725, R² = 0.0514
Area 3: y = 0.0017x + 1.5067, R² = 0.0138
Area 4: y = 0.0033x + 1.6022, R² = 0.0791
y = 0.005x + 0.907
R² = 0.1652
Interdune width (km)
Distance from fixed point at dune-field centre (km)
d
Interdune length versus orientation
Area 1 Area 2 Area 3 Area 4
Interdune orientation (deg.)
Distance from fixed point at dune-field centre (km)

Supplementary 1

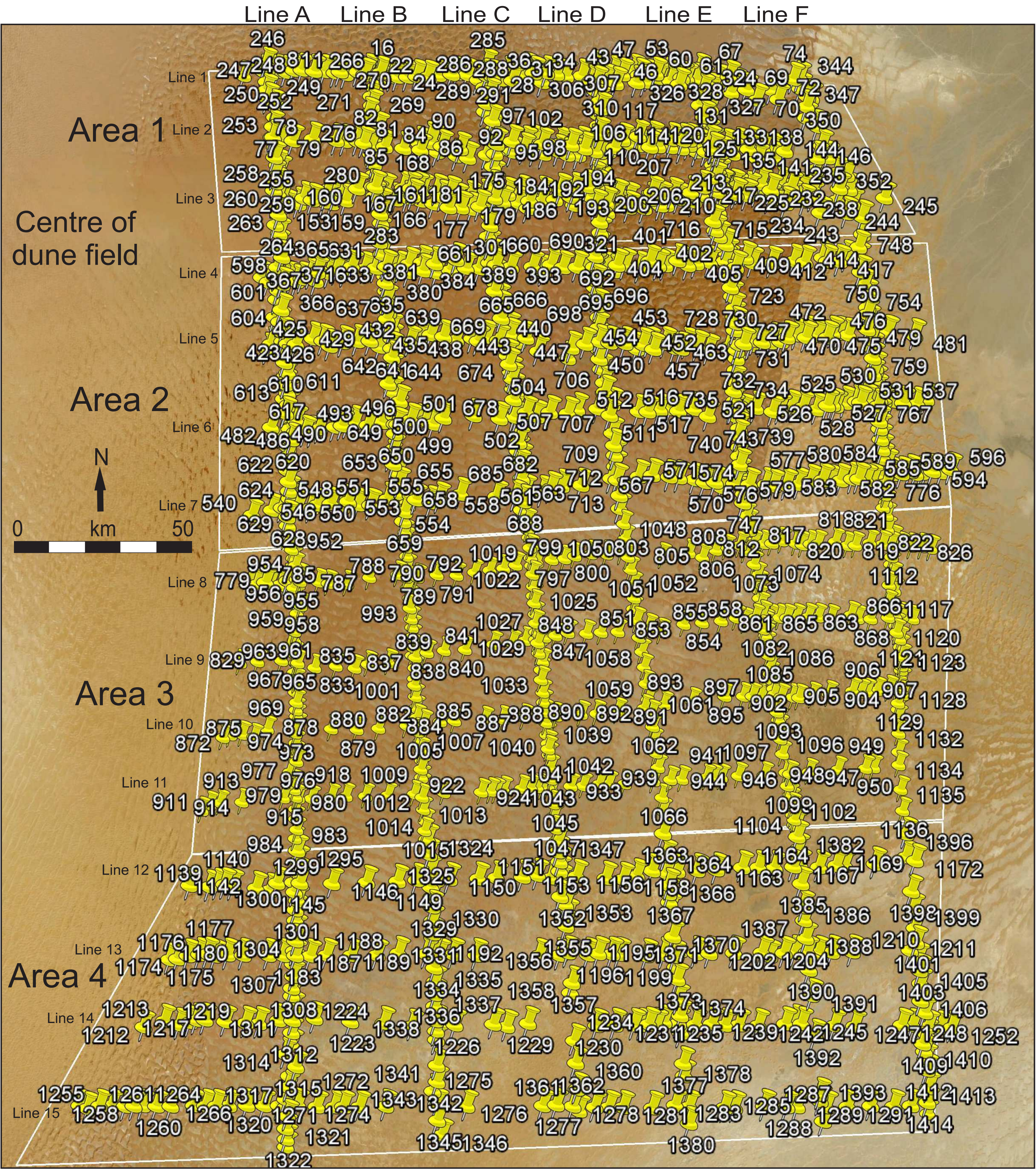

Supplementary 2

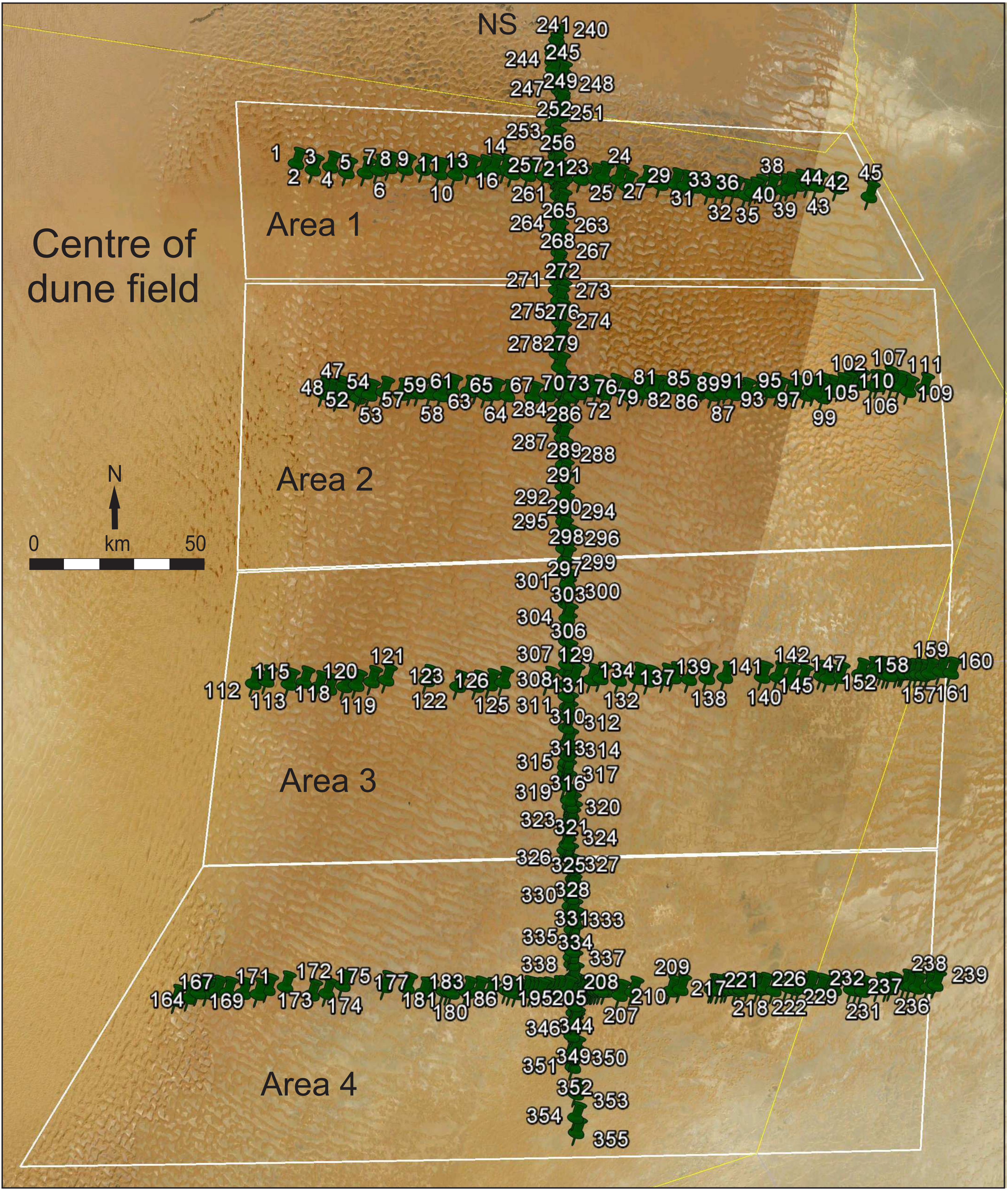

Supplementary 3